Effects of nanosilver on *Daphnia magna* and *Pimephales promelas*

A THESIS SUBMITTED TO THE FACULTY OF
THE GRADUATE SCHOOL OF THE UNIVERSITY OF MINNESOTA BY

Sarah M. Hoheisel

IN PARTIAL FULFILLMENT OF THE REQUIREMENTS
FOR THE DEGREE OF
MASTER OF SCIENCE

Dr. David R. Mount, Adviser

August, 2010

Acknowledgements

Sincere thanks to the UM-EPA Cooperative Training Partnership for giving me the opportunity to complete my graduate study at a world-class government laboratory, and for providing funding to present my results at the 2009 National SETAC meeting.

I could not have completed this work without the knowledge and guidance of my academic advisor Dave Mount, who helped focus my research into a cohesive and meaningful thesis. His innovation and broad knowledge of experimental methods have been critical in the development of many of the techniques described in this document.

Steve Diamond, my technical advisor was as much a part of this study as my academic advisor, offering his expertise during every stage of this project from the preliminary studies to editing the final document. His participation in the international nanotoxicology community has been vital to the accomplishments described in this thesis.

My gratitude goes to the other members of my thesis committee, Rich Axler, Gary Ankley and Pat Schoff, for your enthusiastic support of my proposal and thesis and your generosity with your time.

A group of scientists from the EPA in Cincinnati, OH. including Thabet Tolymat and Amro El Badawy added to my preliminary studies by providing citrate-capped nanosilver and the method to synthesize it.

I owe much to the outstanding scientists at the Duluth EPA laboratory, especially those who assisted with the chemical analyses, including Correne Jenson, Leroy Anderson, and Joe Fernandez, as well as those who stopped in the hallway to express their interest in my project. Russ Erickson was indispensable for his help with the statistical analysis of my results.

Many thanks to Amanda Brennan for helping me find my way around the laboratory, collaborating with me on the preliminary studies, for being an extra set of hands when they were needed, and for your friendship and support.

Dedication

This project is dedicated to my friends and family, whose constant support has been extremely valuable during my graduate studies.

Abstract

The increasing use of nanosilver in consumer products and the likelihood of environmental exposure warrant investigation into the toxicity of nanosilver to aquatic organisms. A series of studies were conducted comparing the potency of nanosilver to ionic silver (Ag^+) at acute and sublethal levels. The results of these tests were examined for evidence that nanosilver acts by a different mechanism of toxicity than Ag^+, with the goal of estimating the adequacy of current water quality regulations based on the toxicity of Ag^+ to protect against environmental effects of nanosilver.

A variety of simple methods to separate Ag^+ from nanosilver by physical exclusion or charge selectivity were assessed in preliminary studies for the ability to provide insight into the mechanism of nanosilver toxicity. In a definitive study, ion exchange resin was used to remove Ag^+ from nanosilver (confirmed by the complete removal of silver from $AgNO_3$ solutions) in order to determine the importance of Ag^+ to acute toxicity of nanosilver to *Daphnia magna*. The acute toxicity of nanosilver to *D. magna* after ion exchange was shown to be similar to that of untreated nanosilver, suggesting that Ag^+ did not contribute significantly to the toxicity of the suspensions, or that ion release occurred rapidly after ion exchange.

D. magna juveniles were exposed to four sizes of nanosilver (10, 20, 30 and 50 nm) and Ag^+ and 48-h LC50s were calculated for each material. Based on mass concentrations, all nanosilver sizes were less acutely toxic than Ag^+, and a trend of increasing toxicity with decreasing average diameter of nanosilver was observed, with LC50s ranging from 19-42 times higher than that of Ag^+. Calculations of nanosilver specific surface area and theoretical surface atoms revealed little to no difference in LC50s among the four sizes, suggesting that toxicity may be dependent on the surface properties of nanosilver. Equivalent calculations for an ionic Ag exposure series resulted in the finding that, in terms of total surface Ag atoms, all sizes of nanosilver were more acutely toxic than equivalent exposures of pure Ag^+. This implies either that a second mechanism of toxicity exists for nanosilver which increases its overall potency, or that the calculation of surface atoms was an underestimate due to the continuous release of Ag^+ from nanosilver into the matrix.

Acute-to-chronic ratios (ACRs) were obtained for *Pimephales promelas* (<24 hours post hatch) exposed to both Ag^+ and nanosilver, to test the hypothesis that a difference in these ratios would indicate different mechanisms of toxicity. The results of 96-h acute and 7-day sublethal toxicity tests produced ACRs for Ag^+ and nanosilver that were not significantly different based on their overlapping confidence intervals. Furthermore, the observation that the nanosilver ACR was smaller than that of Ag^+, suggest that if there is a separate toxicity mechanism in nanosilver, it is unlikely to result in environmental effects beyond those that would be expected from an Ag^+ exposure.

Further studies are needed to determine the degree to which the results of the ion exchange and size-dependent toxicity tests can be attributed to nanosilver dissolution. Overall, the results of these tests do not provide unambiguous evidence for a mechanism of nanosilver toxicity other than Ag^+. The U.S. EPA maximum allowable silver concentration for natural waters is based on dissolved silver, defined as that which passes through a 0.45 µm filter, which is considerably larger than the average size of nanosilver aggregates in the exposure media. Therefore, the presence of nanosilver in the environment will increase the apparent dissolved Ag concentration, resulting in increased protectiveness of this criterion.

Table of Contents

List of Tables

List of Figures

I. Introduction

A. Nanosilver in consumer products: a growing need for environmental toxicology research

The applications for manufactured nanomaterials are contributing to a significant amount of economic growth in sectors including information technology, medicine, construction, and consumer products. It has been estimated that nanotechnology will contribute $10 billion to the global economy in 2010-2015 [1]. Nanotechnology is the manipulation of material on the nanometer scale where unique physical properties make novel applications possible. Nanomaterials can be manufactured into a range of sizes, typically from 1 to 100 nm, and a variety of shapes. The major classes of nanomaterials include carbonaceous nanomaterials such as fullerenes and carbon nanotubes, metallic and metal oxide nanomaterials such as nanosilver, nano-zinc oxide and nano-titanium dioxide, and semiconductor materials known as quantum dots. The Project for Emerging Nanotechnologies has produced an inventory of nanotechnology-based consumer products, which as of August 2009, has grown to 1015 products. The most common nanomaterial in this inventory is silver, with 259 of the products listed claiming to contain nanosilver, “silver nanotechnology” or “silver colloids” [2]. Although nanosilver has been used as an antimicrobial agent in medical practice and in pesticides for more than a century, new manufacturing techniques now allow the incorporation of nanosilver into a variety of products. Among the new uses for nanosilver are personal care products, cleaning products, appliances, water filters, textiles, food packaging and containers,

medical products, and even dietary supplements, where it is often marketed as a “natural” antimicrobial agent.

The rapid expansion of nanotechnology and its commercial applications is threatening to outpace the research on the potential of adverse ecological and health effects should these materials or their degradation products be released into the environment. Increasingly widespread use of nanosilver in consumer products will lead to an amplified risk of exposure to both ionic silver (Ag^+) and nanosilver in the aquatic environments receiving wastewater effluent. There is evidence that fabrics with embedded nanosilver such as socks have a potential to release silver ions and silver nanoparticles into wastewater when they are washed [3,4]. It has been estimated that nanosilver-embedded plastics and textiles will be responsible for up to 15% of the total silver released into European waters in 2010, with the expectation that the market for these products will increase until 2015 [5].

In order to assess the potential risk of environmental release of nanosilver, its biological effects need to be understood and related to the effects of other forms of silver that occur in the environment. For initial studies of nanosilver, it is logical to make comparisons to Ag^+ in terms of its potency, its mechanism of action, and its behavior in natural waters. The goals of these studies should be to determine whether risks of nanosilver and Ag^+ are different and whether current regulations based on the toxicity of Ag^+ will be adequate to protect against the environmental release of nanosilver. The remainder of this chapter will contain a brief summary of the occurrence and toxicity of silver in the environment, a discussion of the aspects of nanosilver which could

theoretically lead to a different set of toxic effects, and a review of the evidence on the toxicity of nanosilver found in published literature. Lastly, I will outline the experimental framework under which I investigated the potency of nanosilver and its mechanism of toxicity compared to Ag^+.

B. Occurrence and toxicity of silver in the environment

Background levels of total silver range from 1-29 pM (~0.1 – 2.9 ng/L) in seawater and from 5-50 pM (~0.5 – 5 ng/L) in freshwater. Even in highly polluted aquatic environments, silver has rarely been measured at more than 3 nM (~300 ng/L). Wastewater treatment plant effluents are recognized as the primary source of silver to receiving waters. Historically, silver mining, manufacturing, and the photographic industry have been responsible for the majority of silver pollution, with the rise of inexpensive digital cameras resulting in a reduction of the total amount of silver released into the environment. However, the growing popularity of silver nanoparticle-based products seems likely to contribute enough silver to wastewaters to compensate for any decreases due to the changes in the photographical industry [5,6].

Acute toxicity of Ag^+, the most potent form of silver, occurs in laboratory studies at concentrations ranging from 0.01 to 70 µg/L in various freshwater species, making it the second most toxic metal after mercury [6,7]. However, the bioavailability of Ag^+ is greatly reduced by the presence of chelating agents, especially sulfides, dissolved organic carbon, and chloride, found in abundance in natural waters. Therefore, most of the silver in the freshwater environment exists in the less toxic complexed form, and no more than

40% (depending on the relative abundance of silver binding ligands) is present as Ag^+ [8].

The mechanism of acute Ag^+ toxicity in both fish and crustaceans is the inhibition of Na^+,K^+-ATPase at the gills, halting the active cellular uptake of Na^+ and Cl^-, and leading to circulatory failure and death [9-11]. The proportion of gill ATPase inhibition that results in mortality is the same in fish and daphnids [9].

The mechanism of chronic Ag^+ toxicity is thought to be the same as that for acute Ag^+ toxicity. Hogstrand and Wood [10] found that the chronic response to sublethal levels of Ag^+ was identical to the acute response – the impaired uptake of Na^+ and Cl^- was proportional to Ag^+ exposures as low as 5% of the 144-hr LC50 of rainbow trout. During 28-day exposures, both appetite and growth rate were found to be inhibited at 2 µg/L Ag. Chronic toxicity of complexed forms of silver is also thought to be possible, though is not yet well characterized [11].

C. Theories and evidence on the toxicity of nanosilver relative to Ag^+

Nanomaterials have properties related to their size, shape, and surface chemistry that are different from the bulk materials from which they are manufactured – this is what makes them useful in novel applications. However, this implies that they may also induce adverse biological reactions that are unpredicted by the effects of the bulk materials. Interactions between silver nanoparticles and biomolecules could lead to pathways of biodistribution, immune response, metabolism, and clearance that are different from Ag^+. Alternatively, if the mechanism of toxicity is the same in nanosilver and Ag^+, some

properties of nanosilver, especially its size, shape, and surface chemistry, are likely to be related to its toxicity because they may influence the effective concentration of the Ag^+ exposure. In addition, water chemistry parameters such as pH, ionic strength, and dissolved organic carbon are known to affect the surface chemistry and aggregation state of nanosilver and to influence its bioavailability. The following paragraphs briefly describe those properties that are thought to be important in influencing the toxicity of nanosilver, whatever its specific mechanism.

Particle size may influence toxicity because, other parameters being equal, smaller particles are presumably more able to penetrate biological membranes than larger particles. The size of nanoparticles is on the same scale as proteins, antibodies, and other biological macromolecules, so under certain conditions they may pass through cellular and nuclear membranes via direct transport or endocytosis more easily than larger particles of the same material [12,13]. In a study using silver, Morones et al. [14] found that only nanoparticles of 10 nm in diameter or less could physically interact with gram-negative bacteria and exert a toxic effect. It has also been shown that nanosilver has the ability to move through the chorion pore canals of fish embryos and accumulate within the organism [7,12,15,16]. Bar-llan et al. [12] observed a slightly increased toxicity in fish embryos with decreasing silver nanoparticle size, and the same size-dependent effect was found in vitro, with decreasing particle size producing increasingly severe effects on mitochondrial function and membrane integrity [17]. Conversely, Hussain et al. [18] reported a slight decrease in vitro toxicity of nanosilver with decreasing particle size.

Specific surface area and surface-to-volume ratio increase exponentially with decreasing particle size. Likewise, the proportion of atoms displayed on a spherical particle's surface increases an estimated 15-20% when particle diameter decreases from 30 nm to 10 nm [19]. It is likely that surface area and surface atoms are correlated with biological reactivity, and that therefore, the toxicity of nanoparticles is dependent on particle size, shape, and surface chemistry.

The surface chemistry of a nanoparticle - its charge and chemical composition - influences its ability to interact with biomolecules, chelating agents, and other nanoparticles, which in turn may affect its bioavailability. Interactions between nanoparticles may result in the formation of aggregates or agglomerates. Aggregates of particles are more strongly bonded than agglomerates. The surface area of an aggregate will be smaller than that of the combined surface area of the individual particles. Agglomerates are more loosely bound collections of single particles or aggregates, with the resulting surface area identical to that of the combined surface area of the individual components [20]. Unaggregated particles may be more likely to be transported into cells, and may display a larger bioreactive surface area than aggregated particles. The aggregation state and size distribution of a nanomaterial may change depending on conditions of pH, ionic strength, and dissolved organic carbon. In general, nanoparticles have an increased tendency to form associations, as pH decreases and ionic strength and dissolved organic carbon increase in the matrix [21]. Specifically, nanosilver has been found to have decreasing toxicity corresponding to the increased aggregation due to the presence of dissolved organic carbon or increasing ionic strength [22]. Conversely, there

is also some laboratory evidence that dissolved organic carbon in natural waters has the effect of coating silver nanoparticles and decreasing their aggregation, leading to increased toxicity [21,23].

Many methods of nanosilver synthesis include a step that adds a surface coating, capping agent, or stabilizer in order to reduce their tendency to form aggregates. Some of the most common additives to nanosilver include citrate, sodium borohydride, polyvinylpyrrolidone, starch, and bovine serum albumin [15,24]. The presence and type of capping agent influences the aggregation behavior of nanosilver in response to the environmental conditions such as pH and ionic strength, and will therefore affect its toxicity. The surface coating on a silver nanoparticle may either increase its toxicity by maintaining a suspension of individual particles with higher surface area [22], or decrease toxicity by reducing the bioavailability of the nanoparticles. The use of surface coatings, dispersants, or buffers in toxicity testing of nanosilver may maintain its stability and size distribution, thereby increasing the researcher's ability to characterize the exposure completely, but it may also reduce environmental realism. The extent to which coated nanosilver is used in consumer products is unknown.

Definition of the properties of nanosilver that are thought to influence toxicity is a challenge not usually associated with the study of soluble chemicals, but is a crucial step in the interpretation of tests with nanomaterials. Some of the ambiguities and conflicting results in the literature discussed in the following paragraphs may be explained partly by the use of different formulations of nanosilver, the use of capping agents, buffers, and dispersal techniques, such as sonication, or by the lack of complete exposure

characterization. Studies that include complete information on the fundamental properties and chemical environment of exposure will contribute the most to the ultimate goal of predicting nanosilver toxicity.

Short term, acute toxicity of various formulations of nanosilver to aquatic organisms has been reported at concentrations as low as 0.04 mg/L (*Daphnia pulex* adults [25]) and as high as 50 mg/L (*Danio rerio*; zebrafish embryos [15]). Sublethal exposures as low as 0.001 mg/L caused changes in stress-related gene expression in *Oryzias latipes* (Japanese medaka) [26]. The mechanism of toxicity of nanosilver is not agreed upon in the literature, but three possibilities are commonly discussed or implied. (1) Toxicity may be caused directly by Ag^+ associated with the particles. Ag^+ may be left over from the synthesis of the particles, released from the particles, or displayed on the surface of the particles. (2) Nanosilver possesses a unique mechanism of toxicity related to properties that emerge at the nano-scale. The theories on how these properties could influence toxicity have been discussed in the preceding paragraphs. (3) Nanosilver acts to increase the exposure to Ag^+ above that indicated by the dissolved concentration of Ag^+ in the bulk solution. This could be due to interactions between nanosilver and biomolecules or membranes that result in an exposure to a higher concentration of Ag^+ than that in the surrounding media. While this represents a pathway of silver toxicity that may be unique to nanosilver, it is not a novel mechanism of action.

Morones et al. [14] assessed the toxicity of nanosilver and Ag^+ on microorganisms and found that the cell morphology was affected differently by each form of silver. Although the Ag^+ concentration of the nanosilver suspension was found

to be present in sufficient levels to contribute to the toxicity, the authors argue that a novel mechanism of nanosilver toxicity is probable due to the observation that small (1 nm) nanoparticles interact with and penetrate the cell membrane.

Asharani et al. [15] observed delayed hatching rate, decreased heart rate, and phenotypic defects in zebrafish embryos exposed to nanosilver capped with organic compounds (starch and bovine serum albumin) but not Ag^+. Nanosilver was observed via TEM to have penetrated the chorion of the embryos, whereas no such accumulation was visible in ionic silver treatments. The authors conclude, based on this evidence, that there is a unique mechanism of toxicity associated with particulate silver. However, these comparisons were based on exposure to much higher concentrations of nanosilver ($\geq$ 100 mg/L) than Ag^+ (2 μg/L), which may have affected the relative toxicity.

Griffitt et al. [25] measured the dissolved silver portion of nanosilver exposures using 20 nm filters and concluded that the acute toxicity in adult and juvenile *D. rerio, D. pulex*, and *Ceriodaphnia dubia* could not be accounted for by dissolved silver alone. The same group (Griffitt et al. [27]) compared molecular and histological effects on *D. rerio* gills of nanosilver and concentrations of Ag^+ equal to the measured dissolved Ag^+ portion of the nanosilver exposure. They analyzed gill filament thickness and gene expression and found significant differences between equivalent exposures of the ionic and particulate forms of silver. Chae et al. [26] evaluated the changes in expression of stress-related genes in *O. latipes* with exposure to equal mass concentrations of nanosilver and ionic Ag^+ and found a different set of responses for each form. These results have led the

authors to conclude that nanosilver and ionic Ag^+ produce separate mechanisms of toxicity.

Laban et al. [7] measured dissolved Ag^+ in two commercially available nanosilver formulations using filtration, centrifugation, and ICP-MS and determined that the toxicity of nanosilver in *Pimephales promelas* (fathead minnow) embryos could not be entirely accounted for by the presence of dissolved Ag^+ alone. The same authors also compared the toxicity of a sonicated nanosilver preparation to nanosilver that was simply stirred. Sonication was shown to reduce the average size of aggregates as measured by TEM, and to increase the acute toxicity to *P. promelas* embryos tenfold, but not to increase the concentration of dissolved Ag^+. It was theorized that sonication breaks up of aggregates into individual nanoparticles, increasing the specific surface area and bioactivity of the nanosilver suspension. Therefore, it was suggested that the small concentration of Ag^+ released from the nanosilver suspension over the period of the toxicity test may have had an additive effect on the overall toxicity of the exposure, but that the nanosilver may also have exerted a separate mechanism of toxicity.

Some authors have also argued convincingly that there is not enough evidence to suggest separate mechanisms of toxicity for nanosilver and Ag^+, and that the toxic action of nanoparticles is more likely to be due to their delivery of Ag^+. Lok et al. [22] found that the toxicity of nanosilver increased with the addition of Ag^+ to its surface, a condition created by bubbling the nanosilver with oxygen. These authors also showed that small (9 nm diameter) silver nanoparticles were much more toxic, on a mass basis, than larger particles (62 nm diameter), but at the mass concentrations of each size that

exhibited the same level of toxicity, the theoretical number of Ag atoms displayed on the particle surface were also roughly the same. These results, along with the finding that bacteria strains with a resistance to Ag^+ were equally resistant to nanosilver, led to the conclusion that the mechanism of toxicity of nanosilver is identical to that of Ag^+.

Navarro et al. [28] found that both ionic and particulate silver influence toxicity in algae. They measured the ionic Ag^+ concentration of a nanosilver exposure using three methods: diffusive gradients in thin films, ion-selective electrode, and centrifugal ultrafiltration. The determination that the concentration of Ag^+ was not high enough to account for the level of photosynthesis inhibition that was observed implies a separate mechanism of toxicity in the nanoparticles. However, when cysteine, a strong silver ligand, was added, the toxicity of both nanosilver and Ag^+ was removed. This led the authors to conclude that the toxicity of nanosilver is mediated by its release of Ag^+, which may be released only upon contact with cells.

A consensus does exist that nanosilver is less acutely toxic than ionic Ag^+, at least on a mass basis. However, there appears to be valid evidence in favor of two conflicting proposals, that nanoparticles possess a unique mechanism of toxicity, or that all toxicity can be accounted for by the presence or delivery of ionic Ag^+. The third option, that nanosilver simply provides a unique pathway for ionic Ag^+ toxicity, is best supported by the results of Navarro et al. [28], and may account for the findings of other authors who claim that the toxicity of nanosilver is above that explainable by the dissolved Ag^+ portion of the exposure. The difficulty in distinguishing which of these is closest to reality lies in making comparisons between equivalent exposures of nanosilver and ionic

Ag^+. The complex behavior of nanosilver within its chemical environment leads to further difficulties in characterizing the toxicity of nanosilver and its relationship to ionic silver. Adequate understanding of the relationships of nanosilver properties and water chemistry to the toxic response will be the key to predicting the environmental risk posed by nanosilver.

D. Overview of the scope of this project

This master's thesis is intended to expand upon the current literature using standard toxicity tests as well as new methods of evaluation to characterize the relationship of nanosilver toxicity to ionic silver. The following three chapters describe the experiments that were designed in order to provide insight into the following questions:

1) How does the lethal and sublethal toxicity of nanosilver compare to that of ionic silver?
2) Is there evidence that nanosilver acts by different mechanisms than ionic silver?
3) Is there reason to believe that risks from environmental releases of nanosilver would not be adequately addressed by existing regulatory approaches based on the toxicity of ionic silver?

Ideally, one would make separate evaluations of the toxicity of nanosilver and Ag^+, therefore, several methods were also attempted to remove Ag^+ from nanosilver, with limited success. An ion exchange treatment was developed in order to remove Ag^+ from

nanosilver, and the acute toxicity of the treated silver was again compared with untreated nanosilver and Ag^+. This was also intended to provide insight into the question of whether the toxicity of nanosilver is solely due to Ag^+, by testing whether the removal of Ag^+ from nanosilver results in a reduction of its acute toxicity.

Where the ability to make direct observations about the contribution of Ag^+ to the toxicity of nanosilver is limited, indirect approaches may be equally valid. To that end, *D. magna* was exposed to four different sizes of nanosilver (10, 20, 30 and 50 nm nominal) and Ag^+ and the LC50s for each size class were expressed in terms of total Ag mass concentration, specific surface area, and surface atoms per mass unit. These properties are theoretically linked to the nanoparticles' contribution of ionic Ag^+ to the exposure, with decreasing particle diameter leading to exponentially greater surface area, and therefore contributing a higher concentration of Ag^+. The characterization of an exposure in terms of its approximate delivery of ionic Ag^+ allows us to evaluate the likelihood that the toxicity of nanosilver is proportional to its delivery of Ag^+, rather than due to a separate mechanism related to the average size of the nanoparticles.

The role of Ag^+ in the toxicity of nanosilver was also evaluated by comparing the acute and sublethal effect levels of 10 nm nanosilver and Ag^+ to *P. promelas* larvae. It is known the mechanism of chronic Ag^+ toxicity is the same as that for acute Ag^+ toxicity in freshwater fish [10]. Therefore, if the source of toxicity in nanosilver is the silver ion, it is logical to assume that the ratio of Ag^+ LC50 to sublethal EC20 will be the same as that of nanosilver. Differing ratios may provide evidence for a separate mechanism of toxicity in nanosilver.

The experimental framework and results of these studies are discussed in the next three chapters. The final chapter addresses the regulatory implications of our findings in relation to the questions listed above.

II. Development of methods for the separation of Ag^+ from nanosilver including evaluation of acute toxicity

A. Introduction

One of the greatest challenges in these studies is the quantification of the ionic silver (Ag^+) content of nanosilver. The direct comparison of the potency of Ag^+ and nanosilver is only possible if the two components can be evaluated separately. One of the assumptions that informed the early preparations for this masters thesis project was that nanosilver suspensions may contain a concentration of free Ag^+ ions at a high enough concentration to contribute significantly to the toxicity of the suspension. Ideally, a comparison of the toxicity of nanosilver and Ag^+ would be made by physically separating the two components and testing them individually. Another assumption is that the main differences between nanosilver and ionic Ag^+ are charge and size, and that therefore, it should be possible to separate or remove Ag^+ from nanosilver by taking advantage of these differences. Filtration, centrifugation, dialysis, ion exchange, and chelation were initially proposed as separation methods. Filtration and dialysis physically exclude larger particles, and centrifugation forces larger particles into a concentrated pellet, which can be analyzed separately from the supernatant. Ion exchange is a method of separating ions from a matrix based on their differential charge. In a nanosilver suspension, it is expected that ionic Ag^+ has a much higher affinity for the active binding sites on ion exchange resin, and that uncharged nanoparticles will pass through an ion exchange column unaltered. Chelation, or chemical binding of Ag^+ that results in a stable complex,

has also been proposed as way to reduce the bioavailability of Ag^+ within a nanosilver suspension, if it can be assumed that the ligand does not alter the reactivity of the nanoparticles themselves. With sensitive enough instruments, it should also be possible to measure the ionic Ag^+ content of a nanosilver suspension, and either determine whether it exists in a high enough concentration to contribute to toxicity, or to evaluate its concentration before and after the treatment of nanosilver with one of the Ag^+ separation techniques listed above. Some of these methods have been reported in publications on the toxicity of nanosilver, as summarized below.

A number of publications on the toxicity of nanosilver have defined the concentration of Ag^+ within a nanosilver suspension as the concentration after filtration with a 0.02 µm filter. Griffitt et al. [25] measured the dissolved ionic Ag^+ in a nanosilver suspension with filtration and reported that the concentration was much lower than the LC50 of ionic Ag^+, which may indicate that the toxicity of nanosilver was not entirely attributable to the dissolved Ag+. Laban et al. [7] used a similar filtration method to measure dissolved Ag^+ in nanosilver over the course of a 96-h static exposure of zebrafish, and although the Ag^+ concentration was generally higher than the LC50 of Ag^+, the mortality rate was actually lower than expected.

Those publications that report a centrifugation step during the synthesis of nanosilver state that its purpose is to remove leftover impurities as well as Ag^+, but there have been no definitive studies on the toxicity of nanosilver before and after centrifugation to produce information about the contribution of Ag^+ to the overall toxicity

of nanosilver. Most authors simply include an exposure using the supernatant of centrifuged nanosilver in order to demonstrate its lack of toxicity [12,15,16,22].

Navarro et al. [28] added cysteine, a strong silver chelator, to nanosilver and ionic Ag^+ exposures, which effectively decreased the inhibitory effects of both forms of silver on the photosynthetic yield of green algae. This result, together with careful measurements of the Ag^+ concentration of nanosilver as discussed in the next paragraph, was used to infer that the toxic action nanosilver is due to ionic Ag^+ transferred directly to the cell membrane even when the dissolved Ag^+ is not high enough to cause toxicity.

Measuring the Ag^+ concentration in a nanosilver suspension is the most direct way to address the question of the contribution of Ag^+ to toxicity. However, because the silver ion is toxic to aquatic organisms at extremely low concentrations, the precise measurement of Ag^+ concentration against a background of a relatively high concentration of particulate silver is challenging. Low concentrations of Ag^+ in nanosilver suspensions were electrochemically measured using stripping voltammetry by Morones et al. [14], who found that the release of approximately 1 µM free silver ions was sufficient to account for at least part of the toxicity observed in *E. coli*,. Ion-selective electrodes (ISE) have also been used for measuring trace levels of Ag^+ in nanosilver suspensions [28,29], however, the electrode detection limit is usually higher than the toxic dose of Ag^+ for many test organisms, and therefore it cannot be used to determine the contribution of Ag^+ to the toxicity of nanosilver. Diffusive gradients in thin films (DGT) was first described by Davison and Zhang [30] for measuring low concentrations of Ag^+ and later utilized for measurements in nanosilver by Navarro et al.

[28]. A DGT device is composed of a layer each of polyacrylamide gel and ion exchange resin separated from the test water by a dialysis membrane. Centrifugal ultrafiltration has also been used successfully to quantify the dissolved Ag^+ in a nanosilver suspension [22,28,31]. Navarro et al. [28] measured the Ag^+ concentration of nanosilver using three methods (ISE, DGT, and centrifugal ultrafiltration), and reported an average concentration of 1% Ag^+ in the nanosilver preparation. Those authors who report sufficiently precise measurements of Ag^+ in nanosilver suspensions vary in their conclusions about its contribution to toxicity. However, in general they suggest that the Ag^+ concentration is often high enough to contribute to at least some of the toxicity of nanosilver. Therefore, to determine whether nanosilver exerts a unique mechanism of toxicity, the bioavailable Ag^+ component must be completely eliminated.

The purpose of the experiments described in the present study was to briefly explore the simplest methods of Ag^+ separation from nanosilver, and where possible, make comparisons of acute toxicity before and after each treatment. Since this was an exploratory study a wide variety of experimental methods were built progressively, based on the results from preceding experiments. Each procedure will be discussed separately, with the methods and results interspersed with conclusions about the efficacy of each. A final discussion section integrates the results and conclusions of all methods in terms of their contribution to the evidence concerning the mechanism of nanosilver toxicity.

B. Methods, materials, and results

The initial studies reported below used citrate-capped nanosilver that was synthesized in-house (see Appendix A). The effectiveness and technical simplicity of filtration, centrifugation, dialysis, ion exchange, and chelation was explored. Following initially promising results, a more extensive study of the effects of ion exchange on nanosilver toxicity was completed using a commercially available preparation of nanosilver (10 nm Biopure, nanoComposix Inc). The results of these studies on the separation of Ag^+ from nanosilver made it possible to infer the role of Ag^+ in nanosilver toxicity.

Characterization of the nanosilver before and after treatment is important to determine that the only thing that has changed about the suspension is the concentration of ionic silver. Some methods of Ag^+ separation might cause a change in the matrix that leads to aggregation of nanoparticles, which may be detected with dynamic light scattering particle size analysis (DLS; Appendix C) and UV-VIS spectroscopy (Appendix C). With this in mind, water chemistry parameters including pH and conductivity were also monitored and controlled where possible throughout each treatment procedure.

Filtration

Cellulose filters with 0.020 µm pore size (Whatman) were used to filter 72 mg L^{-1} nanosilver (citrate-capped) with measured particle size of 92 (±1.1) nm. The particle size of the nanosilver suspension did not decrease after filtration, indicating that particles larger than 0.020 µm were not excluded by the filter, therefore, this method was set aside.

Centrifugation

Three 5 mL samples of 72 mg L^{-1} nanosilver (citrate-capped) were centrifuged for 60 minutes at 28,000 rpm. The sample became visibly separated with a clear supernatant and a denser region of nanosilver at the bottom, but did not form a stable pellet. A 4.5 mL supernatant fraction was carefully withdrawn and total Ag concentration was analyzed in duplicate with graphite furnace atomic absorption spectroscopy (GFAAS; Appendix D), resulting in a measurement of 1.8 (± 0.38) mg Ag L^{-1}), which represented an average 97.5% reduction from the original concentration of the suspension (72.9 mg Ag L^{-1} ± 0.7). Particle size was measured with DLS in the pre-centrifuged nanosilver suspension, and in the concentrated post-centrifugation nanosilver fraction of the three samples. The particle size in the supernatant was not measurable, presumably because the concentration of nanosilver in the supernatant was below the DLS detection limit of approximately 1 mg Ag L^{-1}. The average of three runs is reported below:

Sample ID	ave. particle size, nm (± SD)
pre-centrifugation	45.9 (± 0.2)
post-centrifugation 1	46.8 (± 0.9)
post-centrifugation 2	46.2 (± 0.7)
post-centrifugation 3	46.0 (± 0.7)

The effect of centrifugation on the acute toxicity of nanosilver on *Oryzias latipes* larvae was examined. A nanosilver preparation was centrifuged as described in the previous paragraph, and a 4 mL supernatant fraction was separated from a 1 mL concentrated nanosilver fraction. The concentrated nanosilver fraction was resuspended in culture water made from 25% moderately hard reconstituted water and 75% deionized

water (25% MHW[1]), and diluted to nominal concentrations of 18, 37.5, and 75 mg L^{-1} nanosilver, both pre- and post-centrifugation. A centrifuged supernatant fraction was included as a control treatment. Five organisms <24 hours post hatch were added to 5 mL of exposure solution in small plastic cups. Exposures were performed in duplicate. Mortality, defined as lack of movement for 30 seconds, was observed at 24 and 48 hours. Exposures were not renewed. Temperature was maintained with a 25° C water bath within an enclosure. Conductivity and pH were measured in the bulk solutions and found to average 0.48 mS and 7.3, respectively. Total Ag concentrations were measured with GFAAS at the time of test initiation and used to calculate LC50 by regression analysis (Toxicity Relationship Analysis Program v. 1.21, U.S. EPA) or the trimmed Spearman-Karber method where the data did not fit the regression model.

Nanosilver settled and accumulated as a black film on the bottom of the exposure chambers in the centrifuged treatments, but not in the chambers containing non-centrifuged nanosilver suspensions. Survival was 100% in dilution water control and supernatant treatment (measured at 3.38 µg L^{-1} Ag). Survival was slightly higher in the centrifuged treatments in than the unaltered nanosilver stock, as indicated by an LC50 (and 95% confidence interval) for centrifuged nanosilver of 9.08 (2.8, 29.41) mg L^{-1} and 2.06 (0.48, 8.75) mg L^{-1} for unaltered nanosilver. The wide, overlapping confidence intervals make it impossible to say whether the toxicity of pre- and post-centrifuged nanosilver was significantly different. Also, this test did not include a sufficient number

[1] This culture water formulation was developed during preliminary studies comparing the toxicity of nanosilver and nano-titanium dioxide ($nTiO_2$). Because $nTiO_2$ had a tendency to agglomerate in water of higher ionic strength, and test organisms were intolerant of water of lower ionic strength, this formula was devised as a compromise.

of test organisms per treatment (*n*) as specified in standard acute toxicity test methods (ASTM Standard E 729 – 88a,1991) to be able to make a definitive conclusion of the effect of centrifugation on nanosilver toxicity. If the measured Ag in the supernatant is assumed to be dissolved Ag^+ removed from nanosilver during centrifugation, it seems insufficient to account for the observed reduction in toxicity post-centrifugation. It is possible that more dissolved Ag^+ did exist in the pre-centrifuge nanosilver, but that the high energy of the centrifuge caused it to reincorporate into less bioavailable nanoparticles, and that this led to a reduction of toxicity. There are three other possible explanations for the observed reduction in toxicity: either the Ag^+ was not completely removed from the nanosilver, or the toxic Ag^+ component of centrifuged nanosilver is reestablished during the exposure period, or the nanosilver retains its toxicity when Ag^+ is removed. Future expansion of this experiment should address the lack of stability evident in the centrifuged nanosilver during the exposure period. Further conclusions about the source of toxicity of centrifuged nanosilver are made in the next paragraph on chelation.

Chelation

The effect of a strong silver ligand, sodium thiosulfate ($Na_2S_2O_3$) on the acute toxicity of nanosilver (citrate-capped) on *Oryzias latipes* (Japanese medaka) larvae was evaluated concurrently with the experiment described in the previous paragraph on centrifugation. Dilutions of pre- and post-centrifuge nanosilver concentrate fraction, as well as a supernatant control, were prepared with 25% MHW. Nanosilver preparations

with nominal concentrations of 18, 37.5, and 75 mg L^{-1} were prepared in bulk and divided into four replicates of 5 mL each, in small plastic cups. Two replicates of each concentration were spiked with 50 µL of 8.5 g L^{-1} $Na_2S_2O_3$ solution for a final concentration of 85 mg L^{-1}. Five <24 hours post hatch larvae were added after thoroughly mixing the thiosulfate solution into the nanosilver preparation. Controls included 25% MHW and supernatant fraction spiked with thiosulfate. Exposures were maintained and mortality was observed as described in the previous paragraph. Survival was 100% in all controls, as well as all thiosulfate-spiked pre- and post-centrifuge nanosilver concentrations and the supernatant. Therefore, the addition of thiosulfate removed toxicity from both the centrifuged nanosilver and the unaltered nanosilver up to the highest concentration tested. If the assumption is made that the chelator removes toxicity by reducing the bioavailability of Ag^+ and not by altering the toxic action of the nanoparticles themselves, these results imply that source of acute toxicity of nanosilver is ionic Ag^+, at least at these concentrations.

Dialysis

A preliminary study was conducted on the efficacy of dialysis as a method for the separation nanosilver and Ag^+. Dialysis membrane pore size (SpectraPor 7) was chosen based on a chart provided by Spectrum Labs showing the approximate relationship between diameter in nanometers and kilodaltons (kDa). A membrane with a molecular weight cut-off (MWCO) of 10 kDa, corresponding to pore size of less than 5 nm, was considered adequate to retain 10 nm nanosilver. High purity cellulose dialysis tubing

with a width of 15 mm was selected because of its extremely low heavy metal content. To prepare a sample for dialysis, a segment of dialysis membrane was sealed with a plastic clip on one end, filled with 10 mL of sample, sealed on the other end, leaving a small air space, and rinsed with deionized water. The sample was suspended in a glass beaker filled with 2000 mL of the appropriate matrix and a magnetic stir bar. The dialysis beaker was placed on a stir plate with its speed adjusted to keep the dialysis membrane rotating freely in a vertical position, and covered with ParaFilm and aluminum foil to prevent evaporation and exclude light for a 48 hour equilibration period. Total Ag was analyzed with GFAAS in the solutions both inside and outside the membrane.

An initial experiment demonstrated the ability of a 10 mg L^{-1} Ag^{+} solution to pass freely from inside the dialysis membrane and come to equilibrium with the matrix outside the membrane. Approximately 82-96% of the expected equilibrium concentration of Ag^{+} was attained both inside and outside the membrane, indicating a 4-18% loss of silver to surfaces in the dialysis system such as the dialysis membrane, glass beaker, plastic clips, or magnetic stir bar.

With the ability for dissolved Ag^{+} to pass through the membrane established, a series of dialysis beakers was set up to evaluate the ability of Ag^{+} to pass through dialysis membrane from nanosilver (citrate-capped). The equilibrium concentration of Ag^{+} will only become established if the solution inside and outside the membrane is iso-osmotic; however, the concentration of free citrate in this nanosilver formulation was unknown. It was assumed that some proportion of citrate molecules were removed from solution during the synthesis procedure and incorporated into the nanoparticles, leaving some

unknown concentration of free citrate in the nanosilver matrix. This was accounted for by weighing the prepared dialysis bags before and after dialysis; a change in weight would indicate an osmotic imbalance. Pre-dialysis nanosilver particle size, UV-VIS absorbance spectra, and total Ag concentration were measured. Four dialysis bags were prepared with 72 mg L^{-1} citrate-capped nanosilver (see Appendix A for synthesis method). Two of the prepared dialysis bags were placed in beakers containing a citrate solution measuring 100% of the maximum free citrate concentration that would be present if none was bound to nanosilver, and two were placed in beakers containing 50% of that concentration. Samples collected from outside the membrane were analyzed for total Ag with GFAAS at 0, 24, and 48 hours. After 48 hours of dialysis, the bags were weighed, and the contents were analyzed for DLS particle size, UV-VIS absorbance spectra, and total Ag concentration.

Table 2-1 summarizes the changes that were observed in post-dialysis nanosilver in both citrate treatments. Treatment "A" refers to the dialysis beakers that contained 100% of the citrate concentration specified in the synthesis method, and Treatment "B" refers to the dialysis beakers containing 50% of that citrate concentration. Total silver concentration inside the bag decreased approximately 50% in treatment A and 24.4% in treatment B. The concentration of silver, presumably Ag^{+}, that passed through the bag into the citrate matrix was measured at an average of 1.8 µg L^{-1} in treatment A and 0.13 µg L^{-1} in treatment B. Accounting for the dilution factor, this corresponds to a loss of 0.5% and 0.03% in treatments A and B, respectively. The concentration of dissolved silver outside the membrane did not account for the full loss of silver inside the

membrane in either treatment; indicating that either that a large amount of silver sorbed onto the surfaces of the dialysis system, or that it settled out of suspension. This loss due to sorption was much greater in nanosilver suspensions than the Ag^+ solutions described previously, and made a mass balance analysis of the dialysis of Ag^+ out of nanosilver impossible.

In addition to a decreased silver concentration, the measurements of particle size, UV-VIS absorbance spectra, and post-dialysis bag weight revealed changes in those aspects as well. The particle size increased approximately 19% and 16% in treatments A and B, respectively, with a corresponding shift in the absorbance peaks from 440 nm to 450 nm. The absorbance intensity also decreased from 2.85 absorbance units (AU) to 1.00 and 1.45 AU in post-dialysis nanosilver treatments A and B, respectively. A comparison of the absorbance spectra of pre-and post-dialysis nanosilver at similar Ag concentrations shows that these changes cannot be attributed to dilution alone. A broadening of the post-dialysis absorbance peak also suggests a change in the optical properties of nanosilver during dialysis (Fig 2-1).

The weight of the dialysis bags in treatments A and B increased approximately 1% and 4.3%, respectively, during dialysis, indicating that a lack of osmotic balance caused movement of water into the bags, but the dilution did not account for the decrease in silver concentration inside the bags. Furthermore, a dark grey film was observed accumulating on the inside of the dialysis bags containing nanosilver, an indication that the particles were no longer in a stable suspension. All of these observations led to the

conclusion that the citrate-capped nanosilver was altered during dialysis to a point where this material was no longer relevant for toxicity studies.

The primary objective of this experiment was to show that Ag^+ can be removed from nanosilver using dialysis by completing a mass balance analysis and/or by testing the acute toxicity of pre- and post-dialysis nanosilver, but neither of these evaluations was possible given the results reported above. Further dialysis studies using nanosilver in a matrix of known composition and concentration would eliminate the variable of unknown osmolarity of citrate in the nanosilver matrix.

Table 2-1 Summary of nanosilver characterization measurements before and after dialysis

Treatment ID	inside [Ag][C], mg L^{-1}	outside [Ag][D], ug L^{-1}	Δ weight [E], g	PS [F], nm	AU [G]
pre-dialysis	66.7	N/A	N/A 7	0.9 ± 1.2	2.85
A 100%[A]	33.3	1.80	+ 0.26	87.3 ± 0.8	1.00
B 50%[B]	50.4	0.131	+1.15	84.7 ± 1.1	1.45

[A] 72 mg L^{-1} nAg dialyzed against 100% citrate
[B] 72 mg L^{-1} nAg dialyzed against 50% citrate
[C] Total Ag concentration measured inside dialysis bag after 48 hours of equilibration
[D] Total Ag concentration measured outside dialysis bag after 48 hours of equilibration
[E] Change in the wet weight of the filled dialysis bag and clips over 48 hours
[F] DLS particle size measurement, average of 3 runs
[G] Absorbance units at peak height

Figure 2-1 Analysis of UV-VIS absorbance spectra of nanosilver before and after dialysis

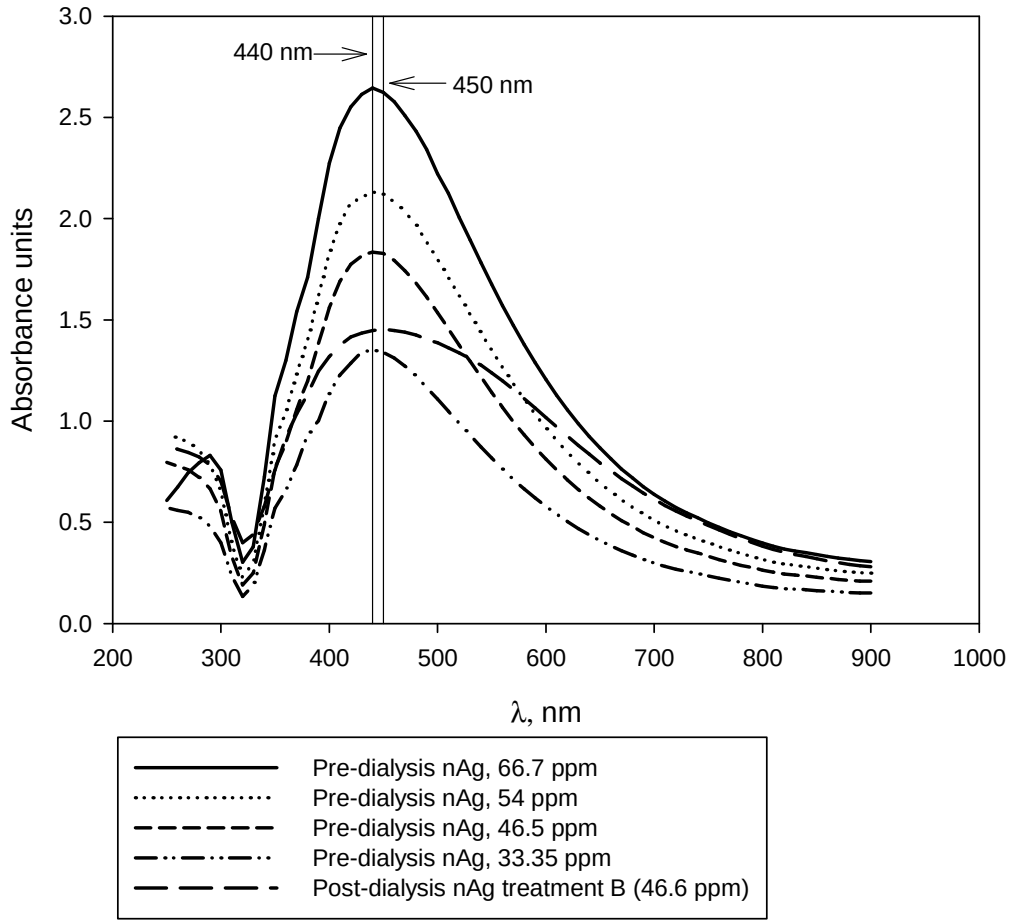

A comparison of pre-and post-dialysis nanosilver peak height at similar Ag concentrations (Pre-dialysis nAg 46.5 mg L^{-1} and post-dialysis nAg treatment B 46.6 mg L^{-1}) shows that the decrease in absorbance intensity in post-dialysis nanosilver cannot be attributed to dilution alone. The wavelength at peak height is 440 nm for each dilution of pre-dialysis nanosilver; the wavelength at peak height is 450 nm for post-dialysis nanosilver. The broadening of the absorbance peak in post-dialysis nAg also suggests a change in the optical properties of nanosilver during dialysis.

Ion exchange part 1, method development and characterization of treated nanosilver

A preliminary study compared the ability of an ion exchange resin to bind silver in both the Ag^+ and nanosilver forms. SIR-300 HP cation exchange resin (ResinTech, West Berlin, NJ has a charge selectivity that theoretically will bind the free Ag^+ component of a nanosilver suspension and not the uncharged nanosilver. Five ml of 15 mg L^{-1} nanosilver suspension was applied to an ion exchange column, prepared and eluted as outlined above. Three mL eluate fractions were collected and analyzed for total Ag by GFAAS.Thirty mg of sodium chloride-activated resin was added to four 200 mL glass beakers. Solutions of Ag^+ (as $AgNO_3$) and a nanosilver suspension of the same mass concentration (0.72 mg L^{-1}) were prepared by dilution in deionized water, and 150 mL of each solution was added to the ion exchange resin. The beakers were placed on magnetic stir plates; samples were collected at 15, 30, 60, and 120 minutes and analyzed for total silver concentration with GFAAS (Appendix D). This batch treatment resulted in nearly 100% of the ionic silver being bound by the resin within 15 minutes, while the total silver concentration of the nanosilver suspensions decreased by only 10-25% in the same period. This indicated that the HP 300 HP resin bound dissolved Ag^+ and left nanosilver, suggesting a promising lead for the development of a method to separate Ag^+ from nanosilver.

This method was refined by utilizing ion exchange columns, which are generally more efficient than batch treatments, and easily allow for the collection of treated samples for further analysis. Commercially available uncapped nanosilver (10 nm in phosphate buffer, BioPure, nanoComposix, San Diego, CA) was used rather than citrate-

capped nanosilver for these tests, because of the extensive characterization data provided by nanoComposix and to allow for the comparison of results among the other studies under the scope of this project (see Parts II and III).

A glass column with a 30 mL bed volume was fitted with a stopcock and filled with 17 mg resin. The resin was activated by pouring five bed volumes of 3% NaCl solution through the column and rinsing with deionized water until the conductivity of the eluate stabilized (measured less than 60 μS). The void volume (10 mL) was approximated by pouring NaCl through the column and measuring the conductivity of the eluate. The capacity for this volume of resin to bind a high concentration of Ag^+ was demonstrated by passing 5 mL of 15 mg L^{-1} Ag^+ (as $AgNO_3$) through the column. After discarding one void volume, the eluate was collected in 3 mL fractions, which were analyzed for total silver by GFAAS. The results showed only trace amounts of Ag remaining in all fractions, which, when diluted, were less than 10% of the 48-h LC50 for *D. magna* juveniles (See Part III). This indicated that, in theory, any ionic silver present in nanosilver could be bound by the resin and whatever passed through the column would be essentially free of ionic silver.

Five mL of 15 mg L^{-1} nanosilver was applied to an ion exchange column, prepared and eluted as outlined above. Three mL eluate fractions were collected and analyzed for total Ag by GFAAS. The fractions with the highest total Ag concentrations were pooled and reanalyzed with GFAAS, DLS, and UV-VIS absorption. A portion of the pooled nanosilver was set aside for toxicity testing, and the remainder was

immediately subjected to a duplicate ion exchange procedure using a new column to determine whether any additional ionic silver was retained.

This procedure was performed three times on separate days, and coincided with two tests of acute *Daphnia magna* toxicity with untreated and ion exchange-treated nanosilver. Mass balance calculations (Table 2-2), include all fractions of eluate collected after nanosilver was passed through the column. Test 1 resulted in an 8.7% reduction in total Ag in post-ion exchange nanosilver; a second ion exchange treatment of the sample was not performed. Test 2 resulted in a 24.7% decrease in total Ag during the first ion exchange treatment, and a further 12.0% decrease when the sample was re-treated 90 minutes later, while the test 3 resulted in 9.6% and 21.5% decreases in total Ag after each of the two treatments, respectively. The variation of Ag reduction from 8.7 to 24.7% is similar to the between-replicate variation of 10-25% observed in the batch treatment ion exchange studies described previously.

It is unknown whether the observed decrease in total Ag after the second treatment of each test reflects the removal of additional Ag^+ that had been released from the particles after the first treatment, or whether it resulted from retention of particulate silver in the column.

Particle size and UV-VIS absorbance data were collected only during test 2 in order to compare these characteristics for nanosilver that was both untreated and subjected to a single ion exchange treatment (See Appendix C for methods). The concentration of the nanosilver after the second ion exchange treatment was too low for particle size and UV-VIS analysis. After the initial treatment with ion exchange, the

average particle size of the nanosilver suspension increased from 38.9 nm pre-ion exchange to 75.3 nm , possibly indicating aggregation in the presence of ion exchange resin. The UV-VIS data show the wavelength at peak absorbance increased from 385 nm pre-ion exchange to 395 (Fig 2-2). These results indicate that both the physical and optical properties of the nanosilver were altered by the ion exchange treatment, although the changes were less significant than the changes observed in nanosilver subjected to other treatments (centrifugation and dialysis).

Table 2-2 Nanosilver ion exchange mass balance

	% decrease in total [Ag]	
Test	Ion ex. treatment 1	Ion ex. treatment 2
1	8.7	N/A
2	24.7	12.0
3	9.6	21.5

Treatment of nanosilver with ion exchange resin columns resulted in a reduction of total silver concentration from 8.7 to 24.7% (Ion ex. treatment 1). A secondary treatment of the same sample nanosilver using a new column (Ion ex. treatment 2) resulted in a further reduction of total silver concentration of 12.0 to 21.5%. This variation is similar to that observed between two replicates of ion exchange batch-treated nanosilver, as described on page 29.

Figure 2-2 UV-VIS absorbance analysis nanosilver before and after ion exchange (Test 2)

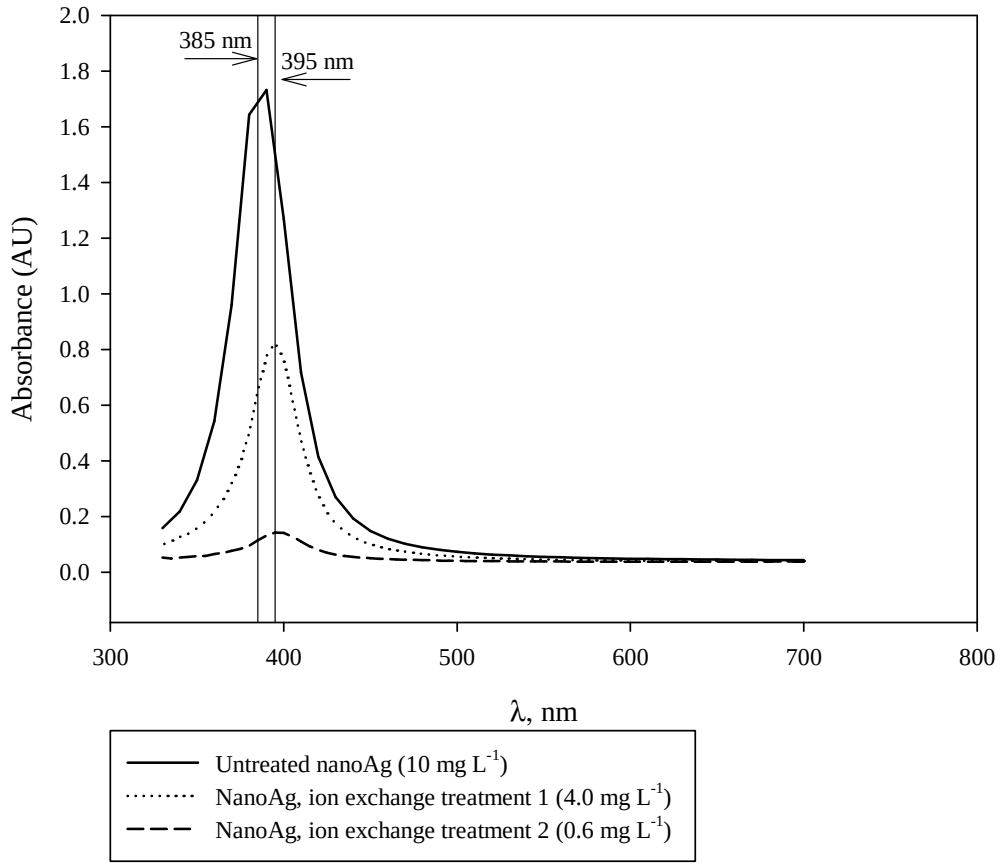

The decrease in peak height in post-ion exchange nAg corresponds to the decrease in Ag concentration; the wavelength at peak absorbance shifted from 385 nm to 395 nm during ion exchange treatment 1. The shape of the peak does not appear to have been altered by ion exchange.. The concentration of the nanosilver after the second treatment was too low for adequate characterization of UV-VIS absorbance.

Ion Exchange part 2, acute toxicity of pre-and post-ion exchange nanosilver

The effect of ion exchange treatment on the acute toxicity of nanosilver was evaluated with 48-h *D. magna* exposures, in order to test the theory that Ag^+ plays a strong role in nanosilver toxicity. If the toxicity of nanosilver is largely due to the presence of Ag^+ in the suspension, and if the free Ag^+ can be removed with ion exchange, and if the nanosilver does not release more Ag^+ during a toxicity test, then it is expected

that ion exchanged nanosilver will have lower acute toxicity to *D. magna* than untreated nanosilver.

The nanosilver formulation that was used for these tests is shipped as a 1000 mg Ag L^{-1} concentrate in a buffer of 2 mM phosphate. Although the concentration of phosphate buffer in post-ion exchange nanosilver is unknown, initial studies confirmed the lack of toxicity to *D. magna* of the phosphate buffer present in nanoComposix Biopure nanoparticles (10 nm), at these dilutions (See Appendix B).

The pooled fractions of nanosilver treated once with ion exchange were serially diluted in filtered Lake Superior water (LSW) in 50% increments to prepare exposures ranging from 1.56 µg L^{-1} to 50 µg L^{-1} (nominal concentration). Untreated (pre-ion exchange) nanosilver was likewise diluted to prepare exposures of the same concentrations. Other treatments included an LSW control and a column blank control, which was produced by passing deionized water through the ion exchange column before adding nanosilver, and diluting the eluate in LSW to the same level as the highest nanosilver exposure. To compare the effects of nanosilver to Ag^{+}, an ionic silver reference treatment was prepared by diluting a 16 mg L^{-1} Ag^{+} solution (as $AgNO_3$) in LSW in 50% increments ranging from 0.25 µg L^{-1} to 4 µg L^{-1}.

The conditions of these acute tests fit the acceptability criteria specified by ASTM Standard E 729 – 88a,1991. All exposures were prepared in bulk and divided into duplicate 30 mL glass beakers filled to a volume of 20 mL. Ten, 3-5 day-old *D. magna* juveniles were collected from the MED culture unit and acclimated to the dilution water for 4 hours before exposure. Samples were collected for total Ag analysis with GFAAS

immediately after adding organisms, as well as at 24 and 48 hours. Beakers were covered with a glass plate and kept on the bench top of a temperature-controlled (temp?) laboratory with a 16:8 photoperiod. Temperature, dissolved oxygen, and pH were measured in one replicate of each concentration of each treatment series per day, using meters (YSI, Inc., Yellow Springs, OH) that were calibrated weekly, and averaged 20.4 °C, 9.10 mg L^{-1} O_2, and 6.64, respectively. Particle size and UV-VIS spectroscopy is not possible at the low concentrations of these exposures (see Appendix C for a summary of particle size behavior at higher concentrations in exposure system matrixes). Exposures were not renewed. Mortality, defined as lack of movement for 30 seconds, was determined at 24 and 48 hours. LC50s were determined with regression analysis (Toxicity Relationship Analysis Program v. 1.2, U.S. EPA) using the average measured exposure concentration.

This test was conducted twice, corresponding with ion exchange mass balance tests 2 and 3 above. During test 2, the organisms showed signs of stress (i.e. poor survival during acclimation period), but the test was completed anyway due to a shortage of healthy organisms. Test 3 was conducted with a normal *D. magna* culture. Despite the perceived differences in the initial health status of the organisms, the LC50s of the Ag^+ reference treatments were almost identical in both tests: 0.40 µg L^{-1} and 0.39 µg L^{-1} respectively (Figure 2-3). An error in dilutions during test 2 prevented a direct comparison of LC50s of pre-and post-ion exchange toxicity. In test 3, the LC50s of pre- and post-ion exchange nanosilver were 2.79 µg L^{-1} and 2.15 µg L^{-1} respectively (Table 2-3).

The purpose of these toxicity tests was to determine the effect of ion exchange treatment on the acute toxicity of nanosilver by comparing the LC50s of pre-and post-ion exchange nanosilver. It is difficult to say whether the LC50s of the pre-and post-ion exchange nanosilver from test 3 are significantly different in a statistical sense, because the variance of these observations is unknown. One simple metric of comparison is the degree of overlap of the 95% confidence intervals for the LC50s; the fact that they do overlap can be used to suggest that they are not significantly different. Another way to evaluate the likelihood that the LC50s are significantly different is to make a reasonable estimate of the variability of LC50s among tests performed under identical conditions. The LC50 for Ag^+ of both tests had less variability (0.40 vs 0.39 ug/L) than the LC50s for post-ion exchange nanosilver (2.79 vs. 2.15 ug/L); therefore we might assume that the difference in LC50 between post-nanosilver tests is within the normal range of variability. Perhaps the most conservative interpretation of these results is that ion exchange does not appear to *greatly* affect nanosilver toxicity, despite the evidence that 100% of ionic silver is removed by ion exchange.

This implies two possibilities for the role of Ag^+ in nanosilver toxicity: either, 1) the removal of Ag^+ has no effect on the toxicity of nanosilver, or 2) Ag^+ can be removed but quickly reestablishes a lethal concentration under the conditions of this toxicity test. If the first possibility is true, it may be either because nanosilver possesses a unique mechanism of toxicity or that nanosilver retains its ability to transfer Ag^+ to biological targets even when no dissolved Ag^+ is present in the matrix. The second option seems likely, given that the endpoint was measured at 48 hours, a considerable length of time

for an acutely toxic concentration of Ag^+ to become reestablished. Given the 48 hour LC50s of Ag^+ in these tests, only 10% to 17% of the total silver would have be present as Ag^+ to account for the observed toxicity in post-ion exchange nanosilver. It is possible that a test with an earlier endpoint can be developed to evaluate the toxicity of post-ion exchange nanosilver before its Ag^+ concentration is reestablished.

Table 2-3 Results of two 48-hr *D. magna* acute toxicity tests with pre- and post-ion exchange nanosilver (10 nm, nanoComposix), with Ag^+ reference treatments

Test	Test substance	48-hr LC50s, µg L^{-1} (95% LCL, UCL)
2	Ag^+	0.40 (0.26, 0.63)
	Untreated nanoAg	not calculable*
	Post-ion exchange nanoAg[A]	4.88 (3.48, 6.85)
3	Ag^+	0.39 (0.35, 0.43)
	Untreated nanoAg	2.79 (2.23, 3.49)
	Post-ion exchange nanoAg[A]	2.15 (1.74, 2.66)

[A]*Post-ion exchange nanosilver used in toxicity tests 2 and 3 corresponds to ion exchange tests 2 and 3 described on pages 29-32. Also see Table 2-2 and Figure 2-2 for characterization data*

**Unable to calculate LC50 for untreated nanoAg exposure series during test 2 due to a dilution error. See dose-response curves in Figure 2-3 for a comparison of the survival in the pre- and post-ion exchange nanosilver treatments from this test.*

Figure 2-3 Concentration-response curves of *D. magna* survival during 48-hr exposure to untreated and ion exchange-treated nanosilver (10 nm, nanoComposix, Inc.)

a) Test 2[A]

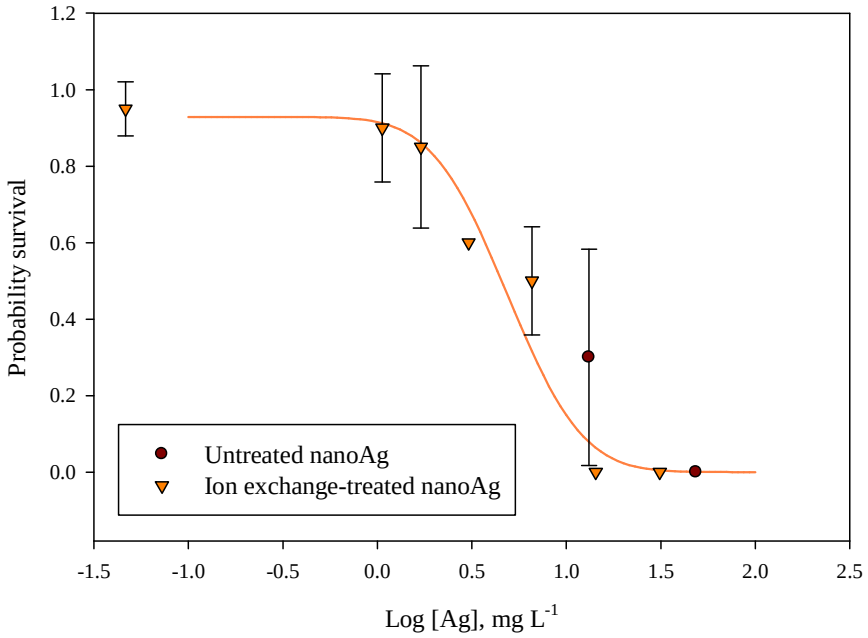

b) Test 3 [A]

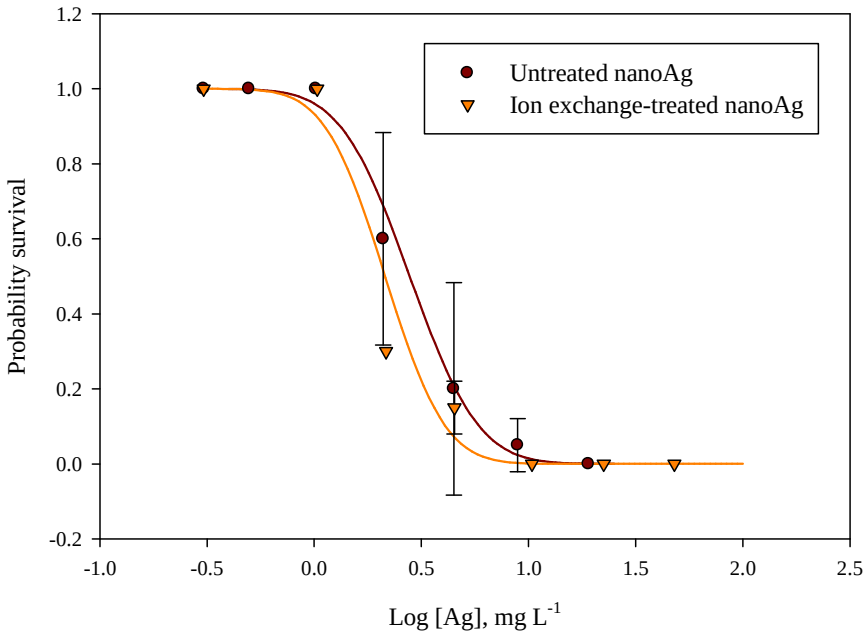

[A]*Post-ion exchange nanosilver used in toxicity tests 2 and 3 corresponds to ion exchange tests 2 and 3 described on pages 29-32. Also see Table 2-2 and Figure 2-2 for characterization data*

Data points and error bars indicate treatment mean ± standard deviation

C. Conclusions and discussion

The effects of filtration, centrifugation, chelation, dialysis, and ion exchange on the character and toxicity of nanosilver have been discussed in terms of their feasibility and likelihood of providing insight into the role of Ag^+ in nanosilver toxicity. Given the limitations of time and resources, those that seemed unlikely to provide these answers were abandoned in favor of more promising techniques, although any one of these could be explored much more extensively. The ambiguity of the results discussed in this chapter led us to investigate indirect, rather than direct methods to compare the toxicity of ionic Ag^+ and nanosilver. The remaining experimental chapters describe tests that focused on the comparison of the toxicity of unaltered nanosilver suspensions and Ag^+ solutions.

III. Particle size-dependent acute toxicity of nanosilver to *Daphnia magna*

A. Introduction

Because it is generally assumed that nanosilver has the ability to release Ag^+, and the results of the tests described in Part II suggest that relatively high concentrations of Ag^+ may become reestablished in nanosilver preparations soon after it has been removed, direct observations of nanosilver toxicity in the absence of Ag^+ may not be possible. An investigation into the acute toxicity of multiple sizes of nanosilver was designed in order to characterize the toxicity of nanosilver in terms of mass concentration, specific surface area and estimated number of particle surface atoms. As discussed in the introductory chapter, it has been theorized that nanosilver toxicity may increase with decreasing particle size, either due to the increased surface area that is available to release Ag^+, a higher particle count, higher effective exposure due to the enhanced ability of smaller particles to penetrate cell membranes, or a combination of any of these.

Evidence for a particle size effect has been reported by Lok et al. [22], Carlson et al. [17] and Bar-llan et al. [12]. Lok et al. compared the antibacterial activity of nanosilver with average particle diameters of 9.2 and 62 nm, and investigated the effect of adding Ag^+ ions to the surface of these particles with an oxygen bubbling technique. They calculated the available Ag^+ in each exposure and found that the antibacterial activity of nanosilver was strongly correlated with the theoretical number of Ag^+ atoms available on the particle surface, concluding that the greater antibacterial activity of the smaller particles was due to the increased surface area-to-mass ratio. Carlson et al. [17]

compared silver nanoparticle sizes of 15, 30, and 55 nm and found no statistical difference in toxicity between 15 and 30 nm particles, but both were significantly more toxic than 55 nm particles in an in vitro study on alveolar macrophages. Bar-llan et al. [12] compared the mortality of zebrafish embryos induced by equal mass concentrations of 3, 10, 50 and 100 nm particles and found increasing toxicity with decreasing particle size. In contrast, Hussain et al. [18] reported that 100 nm nanosilver was slightly more toxic than 15 nm nanosilver in an in vitro study on rat liver cells.

A preliminary range-finding test of acute toxicity in *D. magna* neonates using four nominal sizes of uncapped nanosilver (10, 20, 30 and 50 nm) indicated a clear particle size effect, with toxicity inversely related to size. A definitive experiment was designed in order to compare the 48-hr LC50s of each of these sizes as well as Ag^+ (as $AgNO_3$). The LC50 of each size material was expressed in terms of mass concentration, specific surface area and surface atoms L^{-1}. These surface properties were used to approximate the concentration of available Ag^+ in the exposure, with decreasing particle diameter corresponding to an exponentially greater surface area, and an increasing effective Ag^+ concentration.

B. Materials

BioPure nanosilver preparations were obtained from nanoComposix, Inc. (San Diego, CA) in the form of 1000 mg/L purified, monodisperse suspensions with average particle size of 10, 20, 30 and 50 nm stabilized in a 2 mM phosphate buffer. A commercial source of nanosilver was used for the definitive work reported here rather

than the in-house synthesized citrate-capped nanosilver described in Part II, because the commercial product is of consistent quality, its characteristics are well defined, and it is available in a range of sizes in 10 nm increments. This nanosilver preparation is stabilized with a phosphate buffer to prevent agglomeration and settling, but is not "capped" as is the citrate-capped nanosilver discussed in Part II. The characterization data provided by nanoComposix, including average particle size measured by both transmission electron microscopy (TEM) and dynamic light scattering (DLS), and wavelength at peak absorbance as are outlined in Table 3-1.

Table 3-1 Summary of characterization measurements reported for nanoComposix BioPure nanosilver (10, 20, 30 and 50 nm nominal particle size)

nominal size, nm	TEM dia., nm (SD)[A]	DLS dia., nm (SD)[B]	λ at peak abs, nm[C]
10	10.2 nm (1.7)	not provided	390
20	20.3 (1.9)	27.0 (10.8)	400
30	34.4 (3.4)	42.7 (25.0)	410
50	53.1 (4.1)	57.9 (23.5)	420

[A] Average particle diameter measured by transmission electron microscopy
[B] Average particle diameter measured by dynamic light scattering
[C] Approximate wavelength at peak absorbance; an increase in wavelength of about 10 nm with every 10 nm increase in particle diameter is typical.

C. Experimental design

The conditions of these acute tests fit the acceptability criteria specified by ASTM Standard E 729 – 88a,1991. All test solutions were prepared in bulk and divided into duplicate 30 mL glass beakers filled to a volume of 20 mL. 3-5 day-old *D. magna* neonates were collected from the culture unit (U.S. EPA Mid-continent Ecology Division, Duluth, MN) and acclimated for at least 2 hours in dilution water containing approximately 30 mg L^{-1} of a nutrient slurry (yeast, cereal leaves and trout chow; YCT) before adding 10 organisms to 2 duplicate beakers (n=20 per treatment). Organisms were not fed during the exposure period. Samples were collected for total Ag analysis with GFAAS immediately after adding organisms, and at 24 and 48 hours. Beakers were kept on the bench top in a temperature-controlled laboratory with a 16:8 hour photoperiod, and covered with a glass plate. Temperature, dissolved oxygen, and pH were measured in one replicate of each concentration of each treatment series per day, using meters that were calibrated weekly (YSI, Inc., Yellow Springs, OH), and averaged 20.7 °C, 7.87 mg L^{-1} O_2, and 7.02, respectively. DLS particle size analysis and UV-VIS spectroscopy are not sensitive enough at the low concentrations of these exposures; see Appendix C for a summary of the effects of dilution in exposure matrixes on particle size. Exposures were renewed at 24 hours by filling clean beakers with new exposure stocks and carefully transferring the surviving organisms to the new exposure chambers. Mortality, defined as lack of movement for 30 seconds, was observed at 24 and 48 hours.

LC50s were determined with regression analysis (Toxicity Relationship Analysis Program v. 1.21, U.S. EPA) or with the trimmed Spearman-Karber method where the

data did not fit the regression model. LC50s were calculated based on the average measured exposure concentration and expressed in terms of mass concentration, specific surface area, and the theoretical number of surface atoms per L of nanosilver. Specific surface area and the theoretical number of Ag atoms displayed on the surface of the particles were calculated using the nominal particle size of each exposure series. Surface area of a single particle, *s*, nm^2, was calculated with the formula $s = \pi \cdot r^2$. The specific surface area, $nm^2\ L^{-1}$, was obtained by multiplying the surface area of a single particle by the total number of particles per L, which was calculated using the density of silver (10.5 g/cm^3 at 27°C). The theoretical number of surface atoms, *S*, L^{-1}, was calculated with the formula $S = \frac{6 \cdot Q(N)}{q}$, where *Q* is the diameter of a silver atom (0.25 nm), *N* is the number of atoms per L (based on the average mass concentrations determined by GFAAS measurements during the exposure), and *q* is the nominal particle diameter (Lok et al. [22]). Both of these equations rely on the assumption that all particles in the suspension are spheres of equal diameter, and so are rough estimates.

D. Results

This series of tests was conducted on two separate occasions; the results of each series are identified in the following discussion by their dates. A general trend of increasing toxicity with decreasing particle diameter was apparent in both data sets, when LC50s were expressed in terms of mass concentration (see Table 3-2 and Figure 3-2). The overlap of the 95% confidence intervals (CIs) for the LC50s was used to determine the likelihood that they were significantly different. In test 1, the CIs of the LC50s for 10

nm, 20 nm and 30 nm nanosilver did not overlap, while the 30 nm and 50 nm CIs did overlap. In test 2, only the 50 nm LC50 CI did not overlap with the other CIs, and so appears to be significantly less acutely toxic. A dissolved Ag^+ exposure series was conducted simultaneously with test 2 and resulted in a higher than expected LC50 of 0.98 $\mu g\ L^{-1}$, which may indicate that the daphnid culture was less sensitive at that time, and may explain the higher nanosilver LC50s in test 2 compared to test 1.

Table 3-2 Comparison of 48-hr *D. magna* LC50 (mass concentration) for multiple sizes of nanosilver (nanoComposix, Inc.)

	LC50 (95% CI), $\mu g\ L^{-1}$			
material	Test 1		Test 2	
Ag^+	not measured		0.98	(0.33, unknown)
10 nm	4.31	(3.11, 5.97)	9.60	(7.53, 12.22)
20 nm	8.00	(6.58, 9.72)[A]	13.62	(11.59, 16.00)
30 nm	18.43	(15.78, 21.54)[A]	17.57	(15.15, 20.35)[C]
50 nm	24.48	(20.15, 29.74)[B]	30.36	(26.80, 34.39)[D]

[A]In test 1, the 20 nm and 30 nm LC50 are significantly different from all smaller sized materials, based on non-overlapping confidence intervals
[B]In test 1, the 50 nm LC50 is significantly different with respect to 10 and 20 nm nanosilver only
[C] In test 2, the 30 nm LC50 is significantly different with respect to 10 and 50 nm nanosilver only
[D] In test 2, the 50 nm LC50 is significantly different from all smaller sized materials, based on non-overlapping confidence intervals

Figure 3-2 Concentration-response curves (mass concentration) of *D. magna* survival during 48-hr exposure to multiple sizes of nanosilver (nanoComposix, Inc.)

a. Test 1

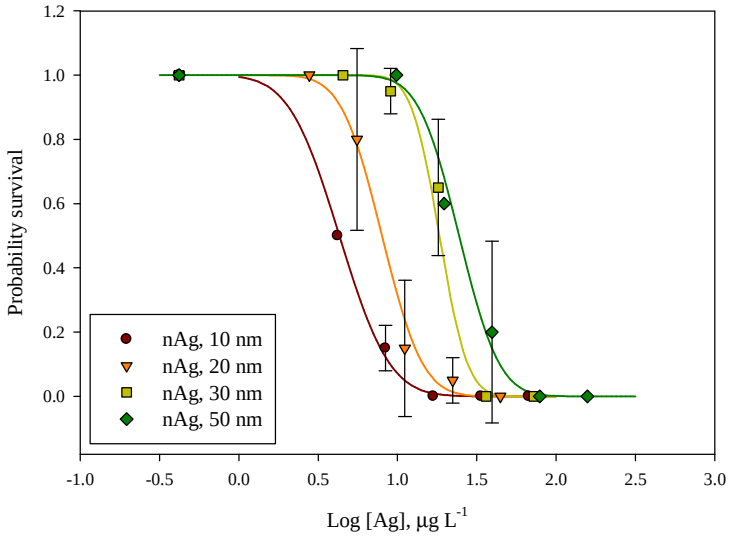

b. Test 2

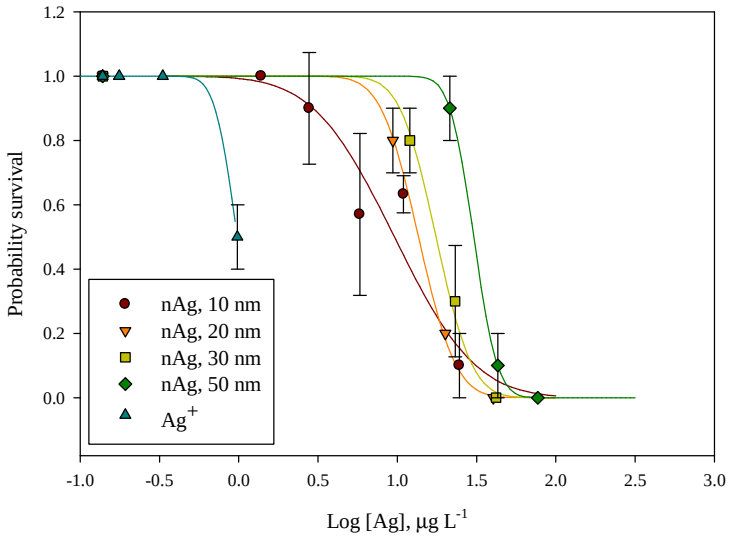

Data points and error bars indicate treatment mean ± standard deviation

When 48-hour LC50s were expressed in terms of specific surface area and number of surface atoms rather than mass concentration of Ag, the toxicity response curves for each size of nanosilver moved closer to one another, appearing to collapse

onto a single curve (Figures 3-3 and 3-4). The LC50s and 95% confidence intervals calculated with surface area and surface atoms exhibited more overlap as well (Tables 3-3 and 3-4). Using either calculation method for both tests, only the test 1 30 nm nanosilver treatment had a significantly different LC50 than the other particle sizes, as estimated by confidence interval overlap (Tables 3-3 and 3-4).

Table 3-3 Comparison of 48-hr *D. magna* 50th percentile effect level (specific surface area) for multiple sizes of nanosilver (nanoComposix, Inc.)

	50th percentile effect level (95% CI), nm^2 L^{-1} x 10^{14}	
material	Test 1	Test 2
Ag^+	NA	NA
10 nm	2.46 (1.78, 3.41)	5.48 (4.30, 6.98)
20 nm	2.29 (1.88, 2.78)	3.89 (3.31, 4.57)
30 nm	3.61 (3.04, 4.30)^A	3.35 (2.89, 3.88)
50 nm	2.80 (2.30, 3.40)	3.47 (3.06, 3.93)

^{A} significantly different from adjacent lower concentration, based on non-overlapping confidence intervals

Table 3-4 Comparison of 48-hr *D. magna* 50th percentile effect level (surface Ag atoms L^{-1}) for multiple sizes of nanosilver (nanoComposix, Inc.)

	50th percentile effect level (95% CI), surface atoms L^{-1} x10^{15}	
material	Test 1	Test 2
Ag^+	not measured	3.29 (1.12, unknown)
10 nm	3.61 (2.60, 5.00)	8.03 (6.31, 10.2)
20 nm	3.35 (2.75, 4.07)	5.70 (4.85, 6.70)
30 nm	5.30 (4.46, 6.30) ^{A}	4.91 (4.24, 5.69)
50 nm	4.10 (3.37, 4.98)	5.09 (4.49, 5.76)

^{A} significantly different from adjacent lower concentration, based on overlap of confidence interval

Figure 3-3 Response curves (specific surface area) for *D. magna* survival during 48-hr exposure to multiple sizes of nanosilver (nanoComposix, Inc.)

a. Test 1

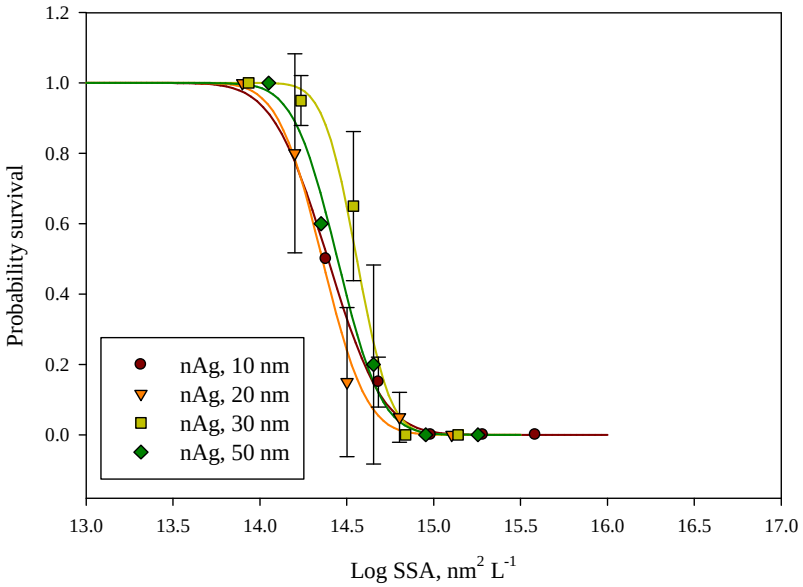

b. Test 2

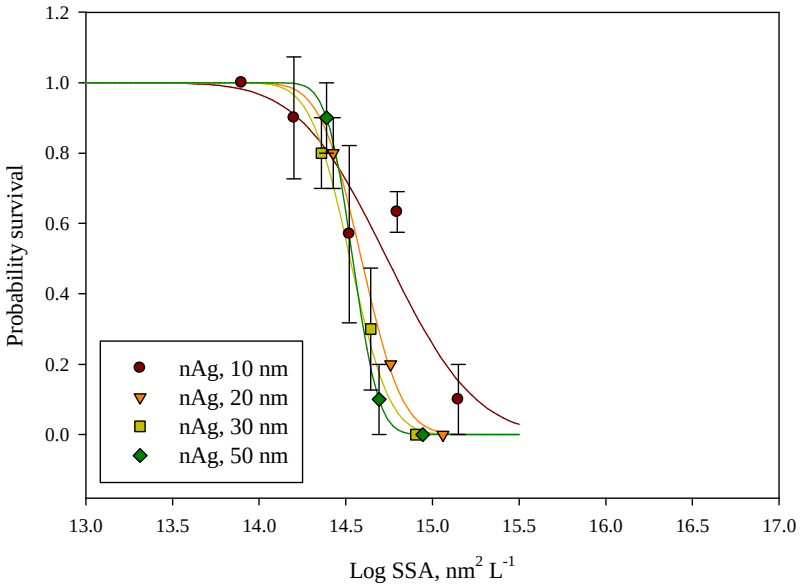

Data points and error bars indicate treatment mean ± standard deviation

Figure 3-4 Response curves (surface Ag atoms L^{-1}) for *D. magna* survival during 48-hr exposure to multiple sizes of nanosilver (nanoComposix, Inc.) and Ag^{+}

a. Test 1

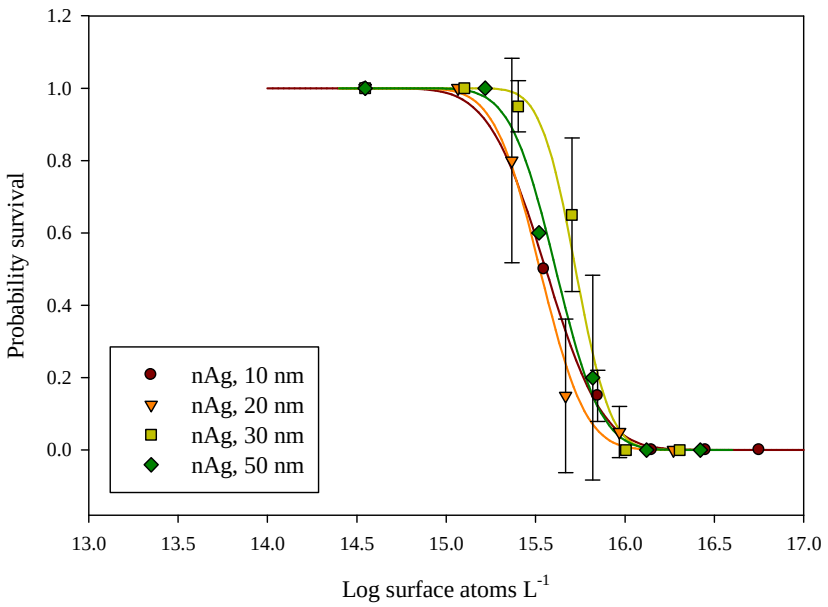

b. Test 2

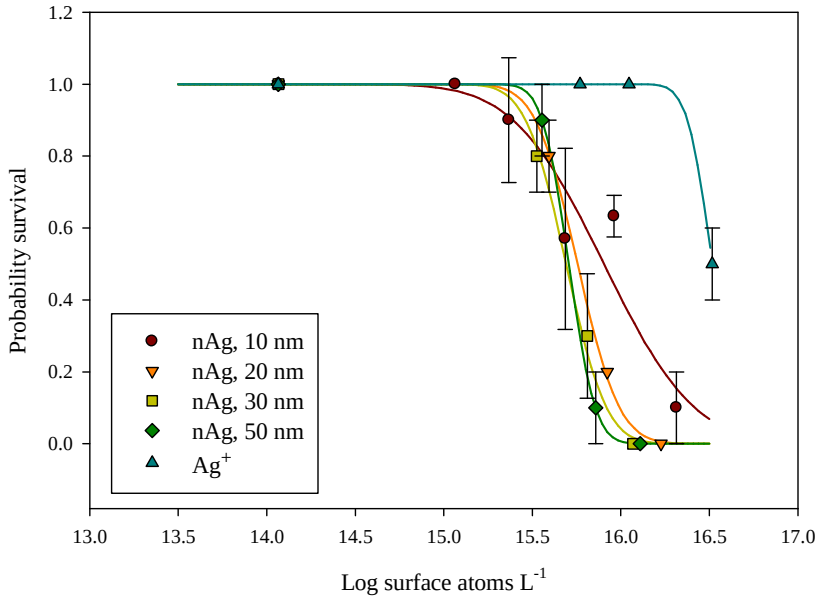

Data points and error bars indicate treatment mean ± standard deviation

The cumulative LC50 based on surface area and surface atoms of all exposures of all sizes was also calculated for both sets of tests. If the LC50 based on surface atoms per L is thought of as an estimation of the total available Ag^+ in the exposure, a direct comparison can be made with the LC50 of dissolved Ag^+, which is simply an exposure in which all silver atoms are equally available. Table 3-5 summarizes the LC50s and 95% confidence intervals of the cumulative exposures calculated by number of surface atoms and the equivalent calculation for the dissolved Ag^+ exposure series. The Ag^+ series resulted in less than 100% mortality at the highest concentration, which prevented the calculation of an upper confidence limit for the LC50. The surface atom LC50 of nanosilver is almost an order of magnitude lower than that of Ag^+, and its confidence interval is spaced well apart from the lower confidence limit of the Ag^+ LC50, leading to the conclusion that they are significantly different (Figure 3-5).

Table 3-5 Summary of cumulative 48-hr *D. magna* 50th percentile effect level (specific surface area and surface Ag atoms L^{-1}) for multiple sizes of nanosilver (nanoComposix, Inc.) and Ag^{+}

	50th percentile effect level (95% CI) x10^{14}	
Exposure metric	Test 1	Test 2
nAg surface area	2.79 (2.53, 3.08) nm^2 L^{-1}	3.87 (3.53, 4.24) nm^2 L^{-1}
nAg surface atoms	40.9 (37.1, 45.1) atoms L^{-1}	56.8 (51.8, 62.2) atoms L^{-1}
Ag^{+} atoms	not measured	329 (112, unknown) atoms L^{-1}

Figure 3-5 Cumulative response curves (surface Ag atoms L^{-1}) for *D. magna* survival during 48-hr exposure to multiple sizes of nanosilver (nanoComposix, Inc.) and Ag^{+}

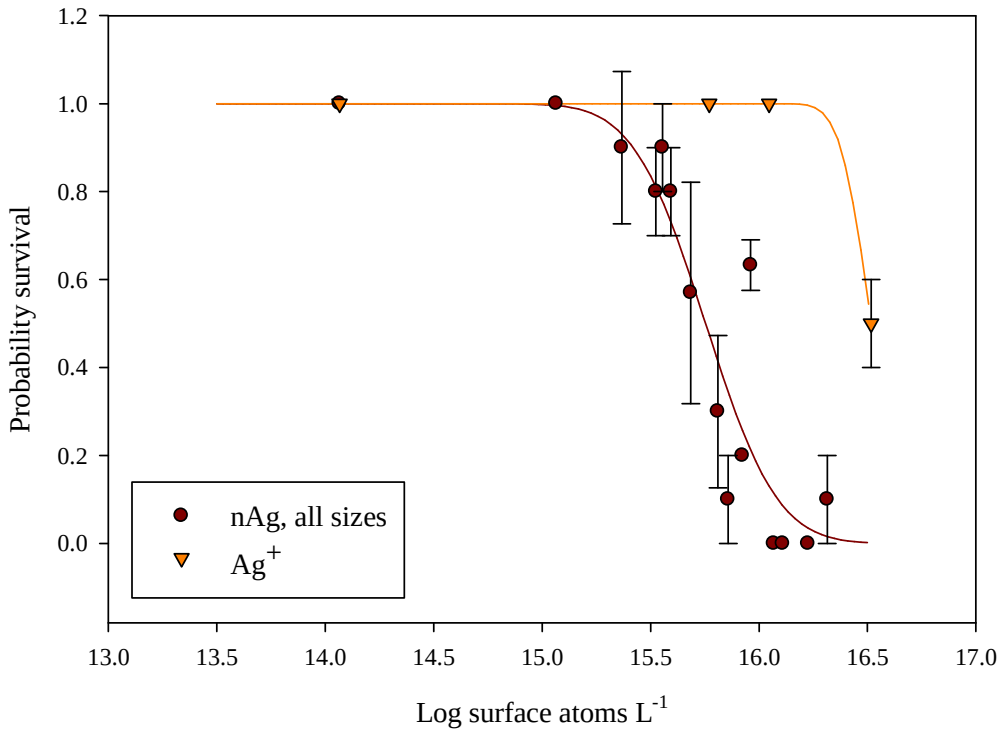

Data points and error bars indicate treatment mean ± standard deviation

D. Discussion

This study found that that Ag+ is approximately 10 times more acutely toxic, on a mass basis, than the smallest size of nanosilver tested (10 nm), in agreement with other publications on nanosilver toxicity [7,22,28]. The size-dependent toxicity of nanosilver demonstrated in the present study is consistent with the findings of Lok et al. [22], Carlson et al. [17] and Bar-llan et al. [12] and is supported by the kinetic model of Liu et al. [31]. The close correlation of acute toxicity with particle surface area is consistent with the hypothesis that Ag^+ released from nanosilver causes toxicity, but it does not eliminate the possibility that another mechanism of toxicity emerges at the nano-scale.

Two possible explanations exist for the observation that, on the basis of surface Ag atoms per liter, nanosilver appears to be more acutely toxic than Ag^+: either 1) nanosilver exerts a mechanism of toxicity beyond that of Ag^+; or 2) the calculated number of surface atoms per liter of nanosilver underestimates the total available Ag^+ throughout the 48-hr exposure period, due to dissolution of nanosilver into Ag^+. One possible explanation for reconciling these hypotheses is that, as suggested recently by a kinetics study by Liu et al. [31], nanosilver gradually dissolves into Ag^+. Liu et al. [31] used centrifugal ultrafiltration to measure the dissolved Ag^+ released from citrate-capped nanosilver at varying levels of initial total silver concentration, temperature, dissolved oxygen, pH, and ionic strength and found that nanosilver completely dissolved into Ag^+ over a period of 6-125 days, with the dissolution rate higher at lower initial Ag concentration. The nanosilver agglomerated with increasing ionic strengh, resulting in an increase of measured particle size from 1.9 to 220 nm, but this did not greatly inhibit the

dissolution kinetics, presumably because the total surface area of the individual nanoparticles was preserved within the agglomerates. Parenthetically, this implies that the use of nominal particle size in my surface area and surface atom calculations is a valid estimation, even though the measured particle size increased significantly due to agglomeration when the material was diluted in the exposure matrix (see Appendix C). However, in light of the published evidence for particle dissolution, it becomes apparent that the surface atom calculation method is only a static estimation of available Ag^+ at a single moment; it does not account for the continuous release of Ag^+ from the particle surface over the 48 hour exposure period, and therefore is likely an underestimate of the number of ionized silver atoms contributing to nanosilver's toxicity.

Liu et al. [31] also found that the addition of natural organic matter (NOM) to nanosilver inhibited dissolution in a dose-dependent manner, possibly resulting from a coating of organic molecules forming on the surface of nanoparticles and blocking oxidation sites, or to the high affinity of organic acids for Ag^+. An empirical kinetic law based on citrate-capped nanosilver results gives an approximation of the rate of Ag^+ release per day per m^2 of particle surface area.

$$-\frac{1}{m}\frac{dm}{dt} = Ae^{-E/TR}\left(\frac{[H^+]}{10^{-7}M}\right)^{0.18} e^{-a[NOM]} \qquad \text{(Liu et al. 2010)}$$

In summary, the results of the present study showing size-dependent toxicity of nanosilver are are consistent with the toxicity studies of Lok et al. [22], Carlson et al. [17] and Bar-llan et al. [12] and supported by the kinetic model of Liu et al. [31]. The close correlation of acute toxicity with particle surface area is consistent with the hypothesis that Ag^+ released from nanosilver causes toxicity, but it does not eliminate the possibility

that another mechanism of toxicity emerges at the nano-scale. The results of Liu et al. [31] imply that the approximations of nanosilver surface area and surface Ag atoms reported in the toxicity tests described here may in fact underestimate the actual Ag^+ exposure, and therefore explain why expressing nanosilver LC50s in terms of surface atoms indicated that nanosilver was more acutely toxic than an equivalent exposure of pure dissolved Ag^+. This illustrates the importance of understanding nanosilver toxicity in terms of dissolution kinetics as influenced by various surface properties and the chemical in defining the relationships between nanosilver characteristics, especially surface properties, and toxicity in terms of the release of Ag^+. The final experimental chapter will describe how the acute-to-chronic toxicity ratio of nanosilver was compared to that of Ag^+ in order to evaluate the likelihood that the mechanism of nanosilver toxicity is identical to that of Ag^+.

IV. Comparison of acute and sublethal toxicity of nanosilver and Ag^+ in *P. promelas*

A. Introduction

This chapter describes the results of concurrent acute and sublethal toxicity tests with Ag^+ and nanosilver that were performed on *Pimephales promelas* (fathead minnow) larvae. These tests were designed to serve two objectives. First, sublethal toxicity characteristics of nanosilver is of fundamental importance, and it is critical to know whether this form of silver produces different sublethal effects than ionic silver. Silver, like most toxicants, is seldom present in the environment at levels that cause acute toxicity, so studies of the sublethal effects of long-term exposures to low concentrations generate more realistic models of the potential toxic effects in natural waters. The determination of more sensitive sublethal endpoints such as growth or reproductive output is therefore useful in linking laboratory toxicity tests with effects at the population and ecosystem level, and for defining unacceptable levels of exposure for regulatory purposes. Concurrent acute and chronic toxicity tests make possible the calculation of acute-to-chronic ratios (ACR), which may then be used to estimate or predict the chronic effect level of the same substance on untested organisms.

Secondly, the comparison of the ACR of Ag^+ to that of nanosilver may provide insight into the mechanism of nanosilver toxicity. It is hypothesized that a different ratio of acute to chronic effect concentration for nanosilver relative to Ag^+ indicates a different mechanism of toxicity. It is thought that the mechanisms of acute and chronic Ag^+ toxicity are the same in fish [10], specifically inhibition of gill Na^+,K^+-ATPase, which

impedes the active cellular uptake of Na^+ and Cl^-. If acute and/or chronic nanosilver toxicity acts by a different mechanism it will likely be reflected by a difference in ACR. Therefore, calculating the ACR for both Ag^+ and nanosilver may provide an efficient method of comparing the toxic response to these two forms of silver, especially in light of the difficulty of removing Ag^+ from nanosilver, as discussed in Parts II and III.

B. Preliminary Studies

In order to maximize the strength of the evidence for or against this hypothesis, it was originally planned to perform acute and chronic tests and calculate ACR for Ag^+ and nanosilver in two model species, *Daphnia magna* and *P. promelas.* However, the ionic silver ACR has been reported as being less than one in daphnids [32,33], because the standard toxicity test protocols give the result that daphnids are less sensitive to silver chronically then they are acutely. This is most likely an experimental artifact caused by the necessity during long term exposures of adding food, a fine-particulate slurry of yeast, cereal leaves and trout chow (YCT), that sorbs ionic Ag^+ and greatly reduces its bioavailability [11].

My preliminary studies confirmed the attenuating effect of YCT on the nanosilver toxicity in *D. magna* neonates (3-5 days old) during a 48-hour exposure (10 nm BioPure nanosilver, nanoComposix Inc.). Static exposures of nanosilver at nominal concentrations ranging from 6.25 to 100 $\mu g\ L^{-1}$ were prepared in 30 mL glass beakers. Two replicates of each concentration were fed at the standard rate of 30 $mg\ L^{-1}$ YCT, and two replicates of each concentration were not fed. Ten healthy organisms were added to

each chamber, which was covered with a glass plate and placed in a temperature-controlled laboratory (25° C air temperature, resulting in an average exposure temperature of 20°±1° C), with a 16:8 hour photoperiod. The exposures were renewed at 24 hours by transferring the surviving organisms to new exposure chambers, with and without YCT. After 48 hours all organisms at the highest fed concentration (100 µg L^{-1} nominal) survived, and the LC50 and 95% confidence interval for the unfed organisms was 19.0 (15.3, 23.5) µg L^{-1}. A separate 48 hour test with Ag^{+} (as $AgNO_3$) fed with YCT resulted in 100% mortality at the highest concentration (31.1 µg L^{-1}; an average of all measurements at this treatment level) and no mortality at the next lowest concentration (14.1 µg L^{-1}), for a fed LC50 of 20.9 µg L^{-1} (no confidence interval available). The unfed exposures resulted in an LC50 estimation and 95% confidence interval of 0.6 (0.46, 0.78) µg L^{-1}. The results of these acute tests, as well as those described in Chapter 3, were used to estimate the acute effect level of nanosilver in the presence of YCT, and led to the conclusion that completing both acute and chronic nanosilver toxicity tests on *D. magna* would be prohibitively expensive.

Further efforts were made to develop an alternative testing procedure whereby YCT was added to the exposures for only four hours prior to each daily renewal. It was reasoned that this pulsed feeding schedule would provide a large window of time during each 24 hour period where nanosilver potency would be unaffected by YCT and therefore increase the sensitivity of the organisms, making lower exposure concentrations possible. However, a control study using this limited feeding regime resulted in poor survival and

growth of *D. magna* neonates, and so the use of this organism in chronic nanosilver tests was discontinued.

Toxicity tests on larval fish are not complicated by silver binding to food, presumably because the brine shrimp nauplii provide a relatively smaller surface area for silver sorption, or a surface with less binding affinity, compared to YCT. This was confirmed in preliminary tests by comparing the survival of *P. promelas* larvae (<24 hours post hatch) with and without feeding in 96-hour exposures to several concentrations of Ag^{+}. Two replicate exposures of 10 larvae at each concentration were fed 3 times daily during the exposure period, while two "unfed" replicates were fed only once at 48 hours. Exposures were renewed daily and measured for total silver with GFAAS (see Appendix D). Ag^{+} concentrations were expressed as the average of three post-renewal measurements taken from each exposure over the course of the experiment. The LC50 and 95% confidence intervals of the fed and unfed exposures, calculated from tolerance distribution analysis using a 3-parameter probit model (Toxicity Relationship Analysis Program v. 2.21, U.S. EPA), were 5.17 (4.14, 6.45) µg Ag L^{-1} for the fed exposures and 3.02 (1.48, 6.16) µg Ag L^{-1} for the unfed exposures. These two results were not significantly different, due to the unusually wide confidence interval of the unfed LC50, and so it may be that the unfed organisms were slightly more sensitive to Ag than those that were fed. Nevertheless, the effect of feeding on the toxicity of silver to *P. promelas* in these tests was very small compared its effect on silver toxicity in *D. magna*, and so it was determined that the comparison of acute (unfed) and sublethal (fed) toxicity tests for *P. promelas* was a reasonable way to obtain ACRs for Ag^{+} and nanosilver.

C. Materials and methods

Acute toxicity tests followed ASTM protocols for conducting acute toxicity tests with fishes, macroinvertebrates, and amphibians (Standard E 729 – 88a,1991). The 7-day fathead minnow EC20 based on survival and growth (EPA-821-R-02-013) was used as a proxy for the chronic EC20 due to limitations of time and materials. This sublethal toxicity test is considered a reasonable estimation for chronic toxicity in *P. promelas* [34,35], and was expected to provide adequate data for the purpose of comparing the ACR of Ag^+ to that of nanosilver,.

The Ag^+ acute and sublethal toxicity tests were conducted first, along with a preliminary acute nanosilver test. The results of these three tests were used to define the range of nanosilver concentrations to produce a range of sublethal growth effects, in order to limit the use of this expensive material during this test. Definitive nanosilver acute and sublethal toxicity tests were conducted concurrently, and each included a single concentration of Ag^+ as a reference treatment, in order to compare the sensitivity of the organisms used in these tests with those used in the earlier Ag^+ tests.

Acute toxicity tests

Exposures were prepared in bulk by serial dilution of stocks of 16 mg L^{-1} Ag^+ or 1000 mg L^{-1} nanosilver (10 nm, BioPure, nanoComposix, Inc) in filtered Lake Superior water (LSW). Stocks with nominal concentrations ranging from 1 to 16 µg L^{-1} (Ag^+) or 25 to 400 µg L^{-1} (nanosilver) were then divided into duplicate 30 mL glass beakers filled to a

volume of 20 mL. An Ag^{+} reference treatment of 8 µg L^{-1} was included with the nanosilver test. *P. promelas* larvae (<24 hours post hatch) were collected from the culture unit (U.S. EPA, Mid-Continent Ecology Division, Duluth, MN) and acclimated to the dilution water in the presence of food for at least 2 hours before adding 10 organisms to each beaker (n=20). Exposure chambers were kept in a water bath at 25° C with a 16:8 hour photoperiod. Mortality, defined as lack of movement for 30 seconds, was determined every 24 hours prior to renewal, and dead organisms were removed. Exposures were renewed every 24 hours by removing approximately 90% of the exposure solution from each beaker and refilling them with new exposure stocks. Organisms were fed a drop of concentrated rinsed brine shrimp nauplii two hours before the 48 hour renewal. Total silver concentration of the new exposure stocks, as well as the 24 hour old exposures was analyzed daily with GFAAS. Temperature, dissolved oxygen, pH, and conductivity were measured in at least one replicate of each concentration per day, using meters (YSI, Inc., Yellow Springs, OH) that were calibrated weekly. DLS particle size analysis and UV-VIS spectroscopy are not sensitive enough to characterize the low concentrations of the nanosilver exposures; see Appendix C for a summary of the effects of dilution in exposure matrixes on particle size. The 96-hour LC50 and 95% confidence intervals were calculated from tolerance distribution analysis using a 3-parameter probit model (Toxicity Relationship Analysis Program, v. 2.21, U.S. EPA).

Sublethal toxicity tests

The test design followed U.S. EPA specifications for 7-day fathead minnow larval survival and growth (EPA-821-R-02-013). Exposures were prepared in bulk by serial dilution of stocks of 16 mg L^{-1} Ag^{+} or 1000 mg L^{-1} nanosilver (10 nm, nanoComposix, Inc) in LSW. Stocks with nominal concentrations ranging from 0.25 to 16 µg L^{-1} (Ag^{+}) or 6.25 to 200 µg L^{-1} (nanosilver) in 50% increments were divided into replicates of four 400 mL glass beakers filled to a volume of 200 mL. The exposure concentrations were chosen to include one that was expected to result in 100% mortality at 96 hours, in order to calculate a 96-hour "fed" LC50 for comparison with the "unfed" LC50 from the acute tests described in the previous paragraph. An Ag^{+} reference treatment of 4 µg L^{-1} was included with the nanosilver test. *P. promelas* larvae (<24 hours post hatch) were collected from the culture unit (U.S. EPA, Mid-Continent Ecology Division, Duluth, MN) and acclimated to the dilution water, in the presence of food, for at least 2 hours before adding 10 organisms to each beaker (n=40). At the start of the test, four groups of 10 organisms were dried in a 90°C oven for 24 hours and weighed to calculate an average initial dry mass per organism. Exposure chambers were kept on a temperature-controlled plate set to 25° C under glass covers in a laboratory with a 16:8 hour photoperiod. Mortality, defined as lack of movement for 30 seconds, was observed every 24 hours prior to renewal, and dead organisms were removed. Organisms were fed with a drop of concentrated rinsed brine shrimp nauplii three times daily. Exposures were renewed every 24 hours by removing approximately 80% of the exposure solution from each beaker and refilling them with new exposure stocks. Total silver concentration of the new exposure stocks, as well as the 24 hour old was analyzed daily with GFAAS

(see Appendix D). Temperature, dissolved oxygen, pH and conductivity were measured in one replicate of each concentration per day, using meters that were calibrated weekly (YSI, Inc., Yellow Springs, OH). DLS particle size analysis and UV-VIS spectroscopy are not sensitive enough for nanosilver characterization at these low concentrations; see Appendix C for a summary of the effects of dilution in exposure matrixes on particle size. At the end of the 7 day exposure period, the surviving organisms from each replicate were rinsed, placed on pre-weighed aluminum pans, and placed in a 90°C oven to dry for 24 hours, then weighed to calculate average dry mass per organism for each treatment level. Average biomass, a cumulative measure of the effects of silver on both survival and growth, was calculated for each replicate by dividing the total dry mass by the number of initial organisms.

The 96-hour LC50s and 95% confidence intervals were calculated from tolerance distribution analysis using a 3-parameter probit model or with the trimmed Spearman-Karber method where the data did not fit the probit model. The 7-day 20^{th} percentile effect concentrations (EC20) and 95% confidence intervals were calculated for each concentration level using both the average dry mass per organism and biomass per exposure chamber from nonlinear regression analysis using a 3-factor probit model (Toxicity Relationship Analysis Program, v. 2.21, U.S. EPA). The sublethal endpoints were normalized to percent of control in order to improve the comparability of tests conducted on separate days. The resulting LC50s and EC20s of these tests were used to calculate ACRs for Ag^{+} and nanosilver.

D. Results

Acute toxicity tests

The conditions of both the Ag^+ and nanosilver acute toxicity tests met the minimum acceptability criteria specified by ASTM (Standard E 729 – 88a, 1991). Control survival was 100% in both tests. Temperature, dissolved oxygen, pH, and conductivity averaged 22.4 (±1.1) °C, 8.3 (±0.2) mg L^{-1} O_2, 7.6 (±0.1), and 111(±3.7) µS, respectively, for the Ag^+ test, and 23.3 (±1.1) °C, 8.5 (±0.3) mg L^{-1} O_2, 7.3 (±0.4), and 110 (±3.9) µS for the nanosilver test.

In the Ag^+ test, the highest concentration (16 µg L^{-1} nominal) resulted in 100% mortality at 96 hours, while the lowest concentration (1 µg L^{-1} nominal) resulted in no mortality. In the nanosilver test, the two highest concentrations (200 and 400 µg L^{-1} nominal) resulted in 100% mortality at 96 hours, while the lowest concentration (25 µg L^{-1} nominal) resulted in 5% mortality. The estimated 96-hour LC50s and 95% confidence intervals for Ag^+ and nanosilver were 4.70 (3.76, 5.89) µg L^{-1} and 89.41 (71.7, 112) µg L^{-1} total Ag, respectively. The 8 µg L^{-1} Ag^+ reference treatment included with the nanosilver test measured an average of 8.03 (±0.05) µg L^{-1} and resulted in 19% mortality (See Figure 4-1 and Table 4-1) and the 8 µg L^{-1} Ag^+ treatment measured an average of 7.44 (±0.23) µg L^{-1} and resulted in 60% mortality.

Figure 4-1 Response curves for *P. promelas* survival during 96-hr exposure to nanosilver (10 nm, nanoComposix, Inc.)

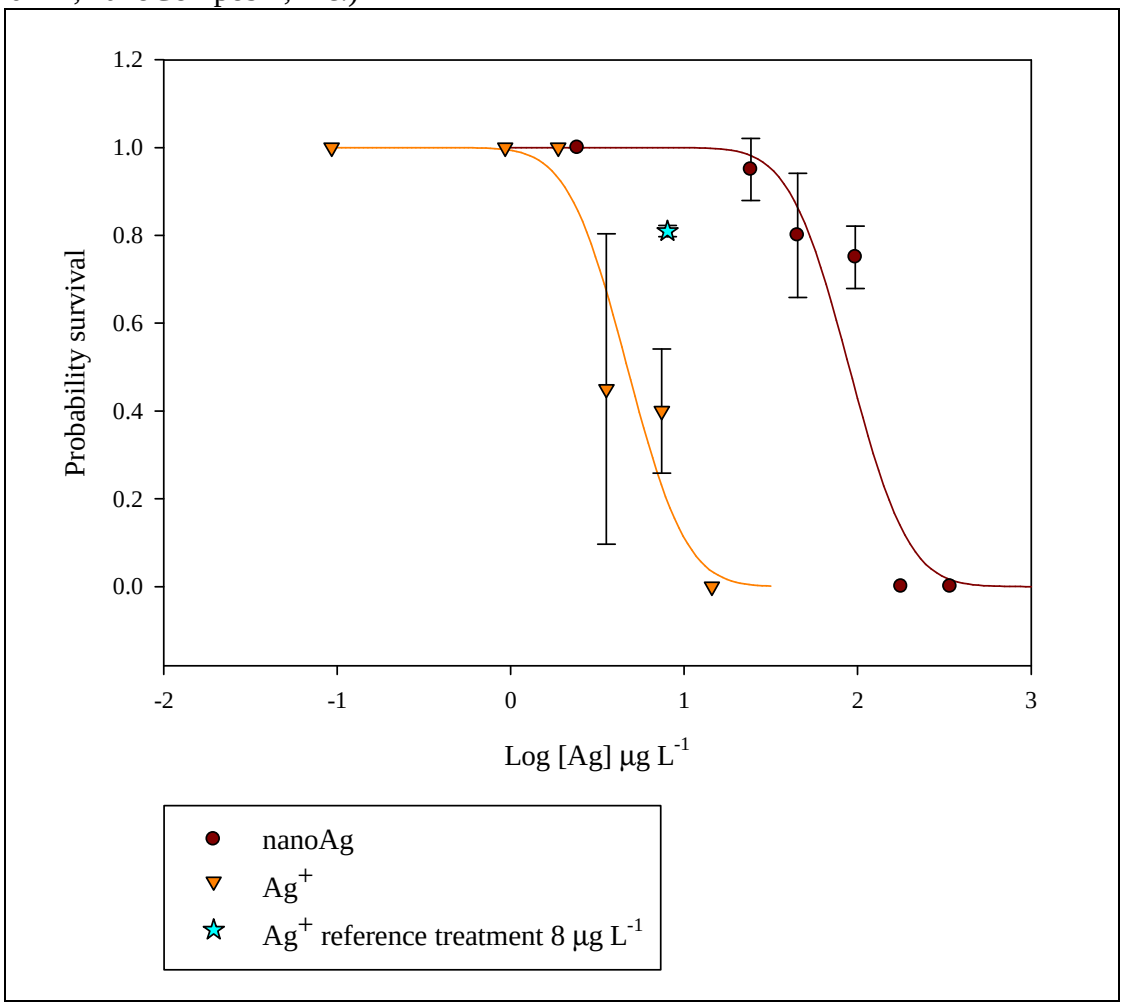

Sublethal toxicity tests

The conditions of both the Ag^+ and nanosilver sublethal toxicity tests met the minimum acceptability criteria specified by the U.S. EPA for 7-day fathead minnow larval survival and growth (EPA-821-R-02-013). Control survival was 90% in the Ag^+ test and 100% in the nanosilver test. Water quality measurements of temperature, dissolved oxygen, pH, and conductivity averaged 23.1 (±1.2) °C, 6.0 (±1.1) mg L^{-1} O_2, 7.1 (±0.2), and 108.28 (±3.75) µS respectively for the Ag^+ test, and 24.0 (±1.2) °C, 6.7 (±0.9) mg L^{-1}, 7.1 (±0.2), and 110.73 (±3.91) µS for the nanosilver test. The increase in average dry mass per control organism from day 0 to day 7 was 0.42 mg in the Ag^+ test and 0.50 mg in the nanosilver test, both of which which exceed the minimum control dry weight criterion of 0.25 mg for the duration of the test.

Consistent dose-dependent reductions in growth and biomass were observed in fish larvae exposed to Ag^+ and nanosilver; both endpoints were found to be similar in statistical sensitivity in both tests. In the Ag^+ exposure series, the highest concentration (16 µg L^{-1} nominal) resulted in 100% mortality, while the next-lowest concentration (8 µg L^{-1}) resulted in 46% mortality. The 96 hour LC50 and 95% confidence interval for the "fed" Ag^+ exposure series was 6.86 (5.75, 8.17) µg L^{-1}. The 7-day LC50 and 95% confidence interval for this exposure series was 5.93 (4.78, 7.35) µg L^{-1}. Average dry weight per organism at 7 days ranged from 93% of control in the 1 µg L^{-1} treatment to 45% of control in the 8 µg L^{-1} treatment. The two lowest concentrations (0.5 and 0.25 µg L^{-1}) resulted in 99% and 101% of the average dry weight of the control group, respectively. The average biomass ranged from to 96% of control in the 1 µg L^{-1}

treatment to 26% of control in the 8 µg L^{-1} treatment (See Figure 4-2). The 7-day dry weight EC20 of Ag^{+} was calculated as 1.37 µg L^{-1} with a 95% confidence interval of 0.59 to 3.20 µg L^{-1}. The biomass EC20 and 95% confidence interval was 1.09 (0.51, 2.35) µg L^{-1} (see Table 4-1)

The 96-h LC50 and 95% confidence interval for the "fed" nanosilver test was 176 (162, 191) µg Ag L^{-1}. The highest concentration (200 µg L^{-1} nominal) in the nanosilver exposure series resulted in 64% mortality at day 7, while the next-lowest concentration (100 µg L^{-1} nominal) resulted in 7.5% mortality. The 7-day LC50 and 95% confidence interval for this exposure series was 152 (131, 178) µg L^{-1}. The average dry weight per organism at 7 days declined from 90% of control to 29% of control over the exposure range of 50 to 200 µg L^{-1}. The 4 µg L^{-1} Ag^{+} reference treatment included in the nanosilver exposure series resulted in 90% of the control dry weight, while 4 µg L^{-1} Ag^{+} resulted in 61% of control dry weight, indicating a decreased sensitivity of test organisms in the nanosilver test. The biomass declined from 90% of control to 11% of control over the exposure range of 50 to 200 µg L^{-1} nanosilver. The 4 µg L^{-1} Ag^{+} reference treatment resulted in 90% of control biomass, compared to 50% of control biomass in the same treatment in the Ag^{+} test (see Figure 3). The 7 day dry weight EC20 of nanosilver was 46.10 (35.07, 60.60) µg L^{-1} and the 7 day biomass EC20 was 50.71 (41.70, 61.67) µg L^{-1} (See Table 4-1).

Figure 4-2 Response curves for *P. promelas* dry mass and biomass during 7-day exposure to nanosilver (10 nm, nanoComposix) and Ag^{+} ; average dry mass and average biomass expressed as percent of control

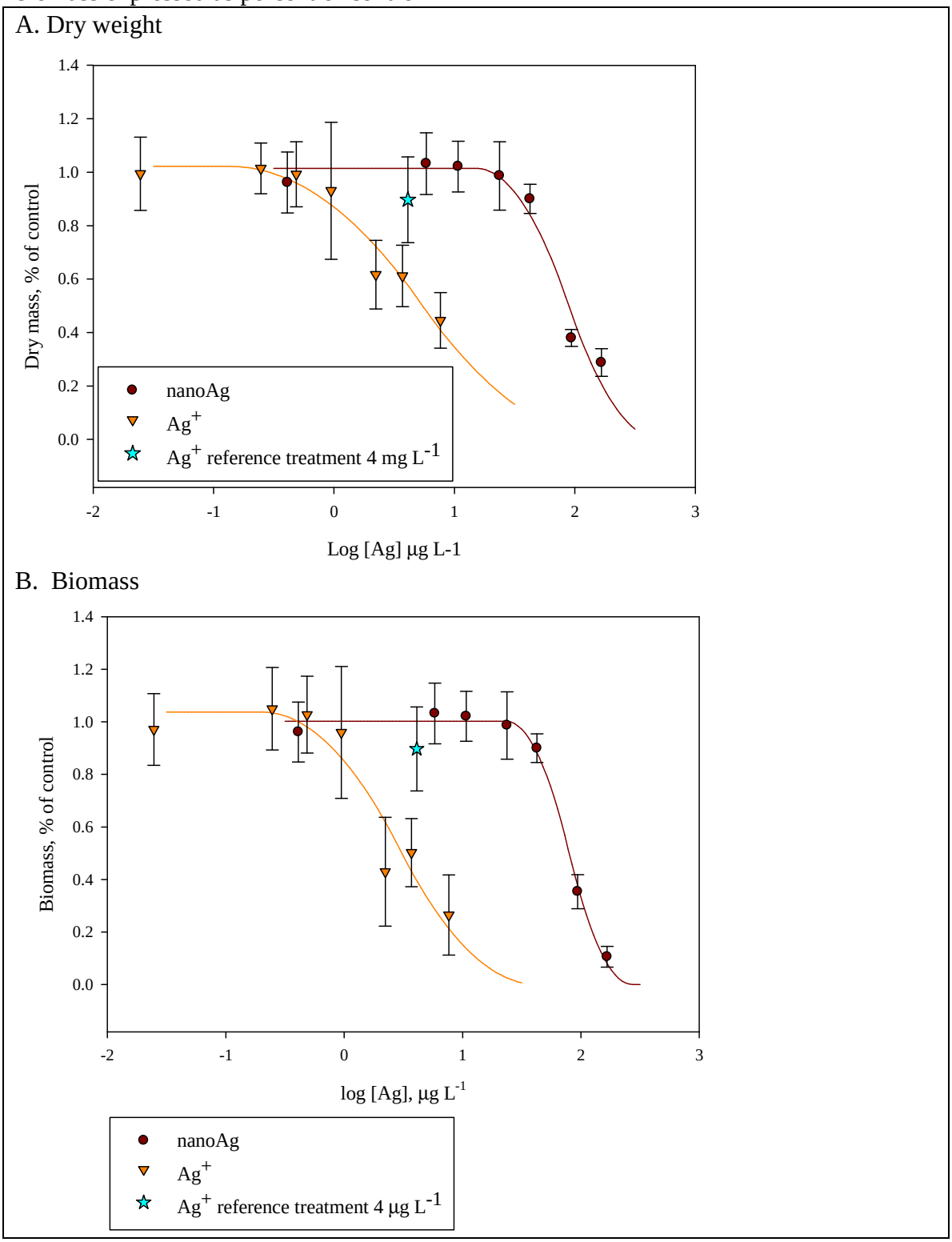

Table 4-1 Summary of 96-h LC50s, 7-day EC20s and acute-chronic ratios for for *P. promelas* larvae exposed to nanosilver (10 nm, nanoComposix) and Ag^+

Test result	Ag^+, µg L^{-1} (95% CI)	nanoAg, µg L^{-1} (95% CI)	
96-h LC50 (unfed)	4.70 (3.76, 5.89)	89.4 (71.7, 112)	
96-h LC50 (fed)	6.86 (5.75, 8.17)	176 (162, 191)	
7-day EC20 (weight)	1.37 (0.59, 3.20)	50.7 (41.7, 61.7)	
7-day EC20 (biomass)	1.09 (0.51, 2.35)	46.10 (35.1, 60.6)	
ACR (unfed:fed)	3.43 (1.42, 5.44)	1.76 (0.44, 3.09)	(weight)
	4.31 (2.42, 6.73)	1.94 (0.67, 3.21)	(biomass)
ACR (fed:fed)	5.01 (3.01, 7.00)	3.46 (2.21, 4.72)	(weight)
	6.29 (4.42, 10.7)	3.81 (2.63, 4.99)	(biomass)

Overlapping CIs indicate no significant difference in ACRs of fed and unfed Ag^+ ACR, based on biomass or weight EC20.

E. Discussion

The results of my acute and sublethal Ag^+ tests were similar to those found in the literature. A study conducted in the same laboratory and using a similar experimental design to that reported here, resulted in an Ag^+ ACR of approximately 8 for *P. promelas* larvae [35]. Others have reported that chronic silver exposures of rainbow trout over 18 months [36] and 6 months [32] have resulted in very high ACRs of 54 and 100, respectively. However, this may be a result of greater sensitivity of this species during such long exposure durations.

Liu et al. [31] described the kinetics of nanosilver dissolution into Ag^+ and concluded that dissolution would continue at environmentally realistic levels of pH and dissolved oxygen over a period of 6 to 125 days, depending on the concentration of dissolved organic matter (see discussion in Chapter 3). However, the effect of nanosilver dissolution in the tests described here is likely to be relatively small, because exposures

were renewed every 24 hours using a nanosilver stock stored in a buffer solution at low temperature to keep it stable.

In order to assess the likelihood that the Ag^+ ACR is significantly different from the nanosilver ACR, the degree of overlap of 95% confidence intervals (CI) of each ratio was examined. The CI for each ACR was calculated using the log of the ratio of the variances of the LC50 and the EC20, and the t-value given for the sum of the degrees of freedom of both tests. This resulted in fairly wide CIs for nanosilver and Ag^+, which do overlap when comparing all combinations of ACRs calculated with both fed and unfed acute LC50s and both dry mass and biomass EC20s. This indicates that although the nanosilver ACRs are relatively smaller, the difference from the Ag^+ ACRs is not significant (Table 4-1). Based on this evidence, there is no strong indication of a different mechanism of toxicity in nanosilver.

The differences in sensitivity of organisms used in the Ag^+ and nanosilver test series illustrate the importance of conducting simultaneous tests for comparative purposes, although this was not practical for this study given time limitations. The organisms used in the acute and sublethal nanosilver tests were appreciably less sensitive than those used in the Ag^+ tests, as indicated by the performance of the Ag^+ reference treatments in the nanosilver tests. This raises the possibility that if all four tests had been conducted simultaneously, either the 7-day weight and biomass EC20s of nanosilver would have been lower, or the 96-hour LC50s of Ag^+ would have been higher. However, because the acute and sublethal tests for each form of silver were performed simultaneously, and any difference in sensitivity would presumably be equally reflected

in the acute and sublethal endpoints, the difference in sensitivity should not influence the resulting ratio of the two endpoints.

The question remains, assuming there is a slight difference in ACR between Ag^+ and nanosilver, whether it indicates a different mechanism of toxicity, perhaps related to the slow-release of Ag^+ or the production of reactive oxygen species (ROS) described by Liu et al [31]. A repetition of these tests to confirm the ACRs of simultaneous acute and sublethal Ag^+ and nanosilver exposures, along with measurements of the dissolved Ag^+ vs. total Ag similar to those described by Liu et al. [31], may shed light on this question. If such a unique mechanism has influenced the results of these tests on the acute and sublethal toxicity of nanosilver to *P. promelas* larvae, its effects must be very small - the sublethal toxicity Ag^+ was 37-42 times greater than that of nanosilver while the ACRs differed by a factor of less than 2. Furthermore, if the ACRs are in fact different, the ACR for nanosilver is smaller than that for Ag^+, suggesting that a separate mechanism is unlikely to result in environmental effects beyond those that would be predicted by the ACR of Ag^+.

A complete summary of the strength of the evidence for a unique mechanism of nanosilver toxicity provided by the other experiments reported in this manuscript follows in the final chapter, as well as a discussion of whether, if a small difference in toxic mechanism exists, different regulatory standards are warrented for environmental releases of nanosilver and Ag^+.

V. Summary and conclusions

A. Review of the purpose and results of these studies

If the properties of nanosilver that differ from ionic silver (Ag^+) lead to a different mechanism of toxicity in aquatic organisms, the water quality criteria for silver may not be adequate to prevent the toxic effects of a release of nanosilver into natural waters. The central questions addressed by this study have to do with the relative potency of nanosilver compared to Ag^+, and whether it produces toxicity by a different mechanism than Ag^+. I have designed experiments intended to detect the presence of toxic effects of nanosilver beyond those that can be ascribed to Ag^+, using ion exchange to separate Ag^+ from nanosilver, by correlating toxicity to the approximate delivery of Ag^+ by multiple sizes of nanosilver, and by comparing the acute-to-chronic toxicity ratios of nanosilver and Ag^+ for a zooplankter and a planktivorous fish Direct and indirect evidence that the toxic effect of nanosilver is proportional to the presence of Ag^+ was considered in this evaluation of the hypothesis that nanosilver toxicity is due to the presence of ionic silver.

Most publications research on the toxicity of nanosilver have included methods to separate Ag^+ from nanosilver or to measure the concentration of dissolved Ag^+ in nanosilver, although few contain convincing evidence on the role of Ag^+ in nanosilver toxicity. In my studies the charge selectivity of ion exchange resin proved valuable in separating Ag^+ from nanosilver, a method which, to my knowledge, has not been previously published. The other methods that I attempted to adapt for this purpose (filtration, centrifugation, chelation and dialysis) may have proven successful with further

development, but were set aside due to limited time and resources. Of the publications that have described these and other methods of separating Ag^+ from nanosilver, or for measuring it, Navarro et al. [28] provides the most substantial argument that the source of nanosilver toxicity is Ag^+, using the silver ligand cysteine along with careful measurements of dissolved Ag^+ to parse the effects of Ag^+ and nanosilver on algae photosynthesis. The results of my study on Ag^+ removal from nanosilver did not allow a comparable conclusion, because the treatment with ion exchange resin did not significantly decrease the acute toxicity of nanosilver to *D. magna*, as would be expected if the source of nanosilver toxicity was Ag^+. This implies either that the nanoparticles continued to release dissolved Ag^+ (as reported by Liu et al. [31]), or to deliver Ag^+ by direct association with cells (as suggested by Navarro et al. [28]), or that nanosilver possesses another mechanism of toxicity. This last possibility seems unlikely, given the nearly identical LC50s of nanosilver before and after treating it with ion exchange. However, without direct measurements of dissolved Ag^+ before and after the ion exchange treatment of nanosilver, the unambiguous interpretation of these results is not possible.

Comparisons of the toxicity of multiple sizes of nanosilver have been published by several researchers in general terms but only one used them to produce evidence about the mechanism of nanosilver toxicity [22]. My studies compared the potency of uncapped nanosilver (nanoComposix, Inc.) to that of Ag^+ using 48-hr acute *D. magna* exposures, 96 hour acute *P. promelas* exposures, and 7-day sublethal *P. promelas* exposures. In terms of mass concentration, nanosilver with nominal diameters of 10, 20,

30, and 50 nm were increasingly less toxic with increasing size, but all sizes were less toxic than Ag^+. In concurrent tests, the 48-hr *D. magna* LC50 for 10 nm nanosilver was approximately 7-10 times greater than that of Ag^+. The 96-hr *P. promelas* LC50 for 10 nm nanosilver was approximately 19 times greater than that of Ag^+. As measured by sublethal endpoints, the 7-day *P. promelas* EC20 for weight was 37 times greater for 10 nm nanosilver than Ag^+, and the EC20 for biomass was 42 times greater for nanosilver than Ag^+. These results agree with the conclusions of Carlson et al. [17] and Bar-llan et al. [12], who found that the smaller of two sizes of particles were more acutely toxic on a mass-basis, but conflict with the results of Hussain et al. [18], who observed a slightly increased toxicity in larger particles.

A study by Lok et al. [22] compared two sizes of nanosilver, correlating toxicity with the presence of chemisorbed Ag^+ on the surface of the particles as quantified by a theoretical calculation of the number of surface atoms. My study described in Chapter 3 included this same calculation for a series of concentrations of four sizes of nanosilver, as well as Ag^+ (as $AgNO_3$). This produced a range of concentrations of approximate Ag^+ delivery by both nanosilver and $AgNO_3$ which were used to compare the 48-h LC50 of both forms of silver on the same terms. The finding that, in terms of total surface Ag atoms, all sizes of nanosilver were much more acutely toxic than equivalent solutions of pure Ag^+, implies that either a second mechanism of toxicity exists for nanosilver which increases its overall potency, or that the calculation of surface atoms was an underestimate due to the continuous release of Ag^+ from nanosilver into the matrix. The results reported by Liu et al. [31] support the interpretation that dissolution of nanosilver

into Ag^+ is a likely explanation, but without direct measurements of the Ag^+ component of these exposures, this cannot be confirmed. However, a second mechanism of nanosilver toxicity can also not be ruled out by these results. Liu et al. [31] also report that nanosilver dissolution was accompanied by reactive oxygen species (ROS) production in simple matrixes, but they did not address this as an additional source of nanosilver toxicity in more environmentally realistic matrixes.

The final method I used to assess the mechanism of nanosilver toxicity was a comparison of the acute-to-chronic ratios of Ag^+ and nanosilver. The ACR is typically used to predict chronic toxicity effects for untested species, but its use as a tool to compare the mechanisms of two related toxic substances where one has some unknown characteristics is less common. To date, there have been no publications on long term sublethal or chronic effects of nanosilver which would allow the calculation of an ACR. The results of my 96-h acute and 7-day sublethal exposures of *P. promelas* produced ACRs for Ag^+ and nanosilver for *P. promelas* that were not significantly different. Although further study is needed to clarify these results, they do not strongly suggest a mechanism of nanosilver toxicity other than Ag^+, or, if there is a separate mechanism, that it would result in environmental effects beyond those expected from Ag^+ exposure. In order to definitively ascribe the results of my studies to nanosilver dissolution into Ag^+, the experiments should be repeated and accompanied by accurate measurements of the dissolved Ag^+ component of nanosilver exposures over the duration of the tests.

B. How well do current environmental regulations address the risk of nanosilver?

The opportunity to evaluate silver regulations before adverse effects of nanosilver are observed in the aquatic environment is timely. A number of countries and international organizations have commissioned research programs with the purpose of informing policy makers on the ability of existing regulations to address the risks associated with an environmental release of nanomaterials. In the United States, the framework of the Toxic Control Substances Act, the Clean Air Act, the Clean Water Act, and the Resources Conservation and Recovery Act all have the potential to enact regulations specifically addressing nanomaterials, as do state-level regulatory agencies.

State silver regulations follow the U.S. EPA ambient water quality criteria for silver published in 1980, which are based on the acute toxicity of Ag^{+}. These specify that the maximum acceptable silver concentration for freshwater, measured as dissolved rather than total silver, is calculated by the formula $10^{(1.72[\ln(hardness)]-6.52)}$, or approximated by half the LC50 [37]. The Lake Superior water used in these tests has a hardness of 45 mg L^{-1} $CaCO_3$, yielding a maximum acceptable silver concentration of 1.07 µg L^{-1}. The results of the toxicity tests reported here indicate that the maximum acceptable concentration of dissolved silver (half the LC50) is 0.20 to 0.23 µg L^{-1} for *D. magna* and 2.35 µg L^{-1} for *P. promelas*. Therefore, based on these data, the hardness-based criterion is somewhat underprotective based on *D. magna* acute toxicity and adequately protective based on *P. promelas* acute toxicity. The existing EPA criterion would be adequate to prevent acute toxicity of nanosilver in either species, given the reduced potency of nanosilver compared to Ag^{+}, by mass concentration.

The definition of dissolved silver for the purposes of this criterion is measured from that which passes through a 0.45 µm filter. Despite the significant agglomeration that occurred under the conditions of these tests, as estimated by measurements described in Appendix C, this suggests that most of the nanosilver in these tests would pass through the filter and be included in the dissolved silver measurement. This increase in the apparent dissolved Ag^+ concentration due to nanosilver would therefore increase the protectiveness of the criterion. Put another way, the simple assumption that all nanosilver in the environment is, or will eventually become, Ag^+, is an overestimation that may be necessary until the mechanism of nanosilver toxicity in relation to its dissolution kinetics are better understood.

C. Suggestions for further study

In addition to the biological effects of nanomaterials, life-cycle analyses are needed for products that contain nanosilver in order to predict the volume of nanosilver that is likely to be released into the aquatic environment, followed by investigations on the fate of nanosilver in wastewater treatment facilities. In wastewater treatment plants with very high levels of dissolved organic carbon, it is likely that nanosilver will be coated in a way that prevents agglomeration and dissolution [31], but this has not yet been tested, and the effects of organic ligands on nanosilver toxicity are not yet agreed upon. Furthermore, the presence of natural aquatic colloids in the same size range of nanomaterials makes the detection of nanosilver in the environment very difficult.

Therefore, the development of a method for quantifying nanosilver in natural waters is a prerequisite for any analysis of risks specifically due to nanosilver.

Investigation of the fate and transport of nanosilver in aquatic ecosystems has barely begun. If nanosilver persists in the environment, even over a period of a few days or weeks, this implies that it may also act as a reservoir of silver, slowly releasing Ag^+ over a longer period of time than other forms of soluble silver that are quickly bound by ligands that reduce their bioavailability [8]. Much is known about the effects of natural chelating agents on reducing the toxicity of Ag^+, but it is unknown whether nanosilver experiences a proportional reduction of toxicity when bound by the same ligands. Studies conducted over a longer period than the 7-day *P. promelas* tests described here are needed to determine whether nanosilver that is taken up by an organism, either by cellular transport or by ingestion, retains its ability to release Ag^+. If this is the case, nanosilver may represent a pathway for Ag^+ toxicity that does not exist for simple complexes of silver. This idea could be tested by comparing the chronic toxicity and accumulation of both Ag^+ and nanosilver, both alone and in the presence of NOM.

Ongoing investigations on conventional forms of silver include chronic toxicity, the toxicity of silver complexes, and the verification of the biotic ligand model for improved site-specific prediction of acute silver toxicity. The results of these studies will have the potential to improve the understanding of the environmental risk of nanosilver, as well as to influence future revisions of the water quality criteria.

APPENDIX

A. Synthesis of citrate-capped nanosilver

The method for synthesizing the citrate-capped nanosilver that was used for preliminary studies was adapted from the well-known Turkevich method for citrate reduction of Ag^{+} by Thabet Tolaymat and Amro El Badawy (personal communication, U.S.EPA, Cincinnati, OH). In this method, the citrate serves as both a reducing agent and a stabilizer which caps the particles and limits their growth and aggregation [38]. Solutions of silver nitrate and sodium citrate were prepared by weighing the compounds and dissolving them in separate aliquots of deionized water. The silver nitrate and citrate solutions were combined and measured into preheated 100 mL volumetric flasks. The flasks were placed in a hot water bath and slowly heated for approximately 2 hours. The UV-VIS absorbance peak was monitored every 30 minutes with a Perkin-Elmer Lambda 20 until it reached an intensity of 2 absorbance units at 400 nm. The particle size was measured with dynamic light scattering (ZetaPALS, Brookhaven Instrument Corp, Holtsville, NY) and found to average 60-80 nm in various batches. The total silver concentration of 72 mg L^{-1} was confirmed using a Varian graphite furnace atomic absorption spectrophotometer (GFAAS, See Appendix D for quantification method). The nanosilver suspension was kept at room temperature (20° C) in a glass flask covered in aluminum foil to reduce light exposure.

B. Citrate and phosphate buffer control studies

Toxicity tests were performed to demonstrate the non-toxicity of the phosphate buffer added to the commercial nanosilver (nanoComposix, Inc) used in the toxicity tests in Parts II, III, and IV. A phosphate stock was prepared as instructed by a representative of nanoComposix, Inc. to match the nanosilver buffer: 62 mg monosodium phosphate and 415 mg disodium phosphate were dissolved in 1 L DIW. Five test solutions ranging from 3 to 48 mg L^{-1} total phosphate were prepared by 50% serial dilutions in filtered Lake Superior water (LSW). Exposures were prepared in duplicate 30 mL glass beakers filled to a volume of 20 mL, including an LSW control treatment.

D. magna juveniles (3-5 days old) were collected from the culture unit (U.S. EPA, Mid-Continent Ecology Division, Duluth, MN) and acclimated for 2 hours in the culture water. Ten organisms were added to each beaker. Beakers were covered with a glass plate and kept on the bench top of a temperature controlled laboratory (20° C) with a photoperiod of 16:8 hours light:dark. Exposures were renewed at 24 hours by preparing new exposure solutions and gently transferring surviving organisms into them. Organisms were not fed. Water quality parameters temperature, dissolved oxygen, pH, and conductivity were measured at 24 hours and averaged 21.0 (±0.1)° C, 8.1 (±0.2) mg L^{-1} O_2, 6.7 (±0.1) and 103.9 (±33.4) µS, respectively. Mortality, defined by lack of movement for 30 seconds, was monitored at 24 and 48 hours.

At 48 hours, the highest phosphate concentration tested (48 mg L^{-1}) had 10% survival, the next lowest (24 mg L^{-1}) had 70% survival, and all other treatments including the controls had 100% survival. The lowest concentration with no acute toxicity at 48 hours (12 mg L^{-1} phosphate), corresponds to a proportional dilution of 1000 mg L^{-1}

nanosilver stock measuring approximately 25 mg L^{-1}. This is 100 times higher than the 48-hr *D. magna* LC50 of 50 nm nanoComposix nanosilver in Part III. Therefore, the acute toxicity of the phosphate component of nanoComposix nanosilver can be disregarded for *D. magna* at these concentrations.

C. Nanosilver characterization under experimental conditions

The characterization of the nanosilver used in these studies was limited to dynamic light scattering (DLS) particle size analysis and UV-VIS absorbance spectra. The DLS method produces an average hydrodynamic diameter based on a very high particle count, but it is susceptible to bias in the presence of dust or large particles. The measure of polydispersity obtained from the DLS method is also therefore associated with a high level of uncertainty. A particle size measurement produced by another common method, transmission electron microscopy (TEM) is based on a much lower particle count, and is prone to error introduced during the preparation of the sample, but it is a measurement of the actual core diameter of the nanoparticles, rather than the hydrodynamic diameter, and produces a reliable measure of polydispersity [39]. The commercial nanosilver used in these studies (nanoComposix, Inc.) was accompanied by a specification sheet that disclosed the TEM particle size and size distribution analysis, as well as UV-VIS absorbance spectra, of each particle size. A comparison of the DLS measurement of particle size to the TEM particle size reported by nanoComposix was therefore a primary objective of these characterization studies.

The presence of a surface plasmon resonance (SPR) peak in the UV-VIS region is a characteristic of nanosilver that does not exist in solutions of Ag^{+}, and is easily detected by UV-VIS absorbance spectroscopy. The characteristics of this peak are commonly used to monitor the agglomeration state of a nanosilver suspension, because the SPR is sensitive to changes in particle size and agglomeration [12,24,40,41].

Because the concentrations of nanosilver in the toxicity tests described in these studies were too low to be characterized by DLS particle size and UV-VIS absorbance spectra, a series of surrogate measurements were made on higher concentrations of nanosilver diluted in experimentally relevant matrixes. The dilution waters tested for their effect on particle size and UV-VIS absorbance peak were deionized water (DIW), filtered Lake Superior water (LSW), phosphate buffer (PHS), and *D. magna* water (DMW). The phosphate buffer was prepared as instructed by a representative of nanoComposix, Inc. to duplicate the buffer in which the 1000 mg L^{-1} nanosilver stock is shipped and stored. A 2 mM phosphate solution was prepared by dissolving 62 mg monosodium phosphate and 415 mg disodium phosphate in 1 L DIW. The DMW was intended to duplicate the chemical composition of 24-hour old exposure chamber containing 20 mL LSW and 10 *D. magna* juveniles. Ten organisms (3-5 days old) were added to 30 mL glass beakers containing 20 mL of LSW and set on the benchtop of a temperature controlled laboratory and covered with glass plates. The organisms were removed before adding nanosilver for characterization.

Preliminary measurements determined that 2 mg L^{-1} nanosilver is the lowest concentration for which reliable DLS and UV-VIS readings can be taken. 1000 mg L^{-1}

nanosilver stock (10, 20, 30 and 50 nm, nanoComposix, Inc) was diluted, in duplicate samples, to 2 mg L^{-1} in 2 mL volumes of each matrix. Each sample was immediately analyzed with DLS and UV-VIS, and then placed in a dark cabinet. Measurements on LSW and DMW diluted samples were repeated after 24 hours. DLS results are expressed as the mean and standard deviation of 6 measurements (3 for each replicate). UV-VIS results for peak absorbance units and wavelength at peak absorbance are given as the average of two duplicate samples.

The most striking result of the particle size measurements (Table A-1) is that the 10 nm nanosilver shows a larger agglomeration effect when diluted in LSW or DMW, compared to the other sizes, and that it is the only material that, when diluted in DIW, does not have a particle size consistent with the nominal size. For all materials, dilution in DMW resulted in slightly larger particle size than dilution in LSW, and dilution in PHS resulted in a slightly larger particle size than dilution in DIW.

The UV-VIS absorbance spectra (Table A-2) of the four nanosilver sizes do not exhibit a great difference whether they were diluted in LSW or DMW. However, a significant change occurs in most materials over 24 hours – the peak height decreased and the wavelength at peak height increased. This may reflect the effect of agglomeration and settling; the absorbance intensity decreases as the particles are removed from the water column, and the remaining agglomerates are larger, resulting in a shift towards a higher wavelength.

Table A-1 Comparison of DLS particle size analysis of multiple sizes of nanosilver (nanoComposix, Inc.) in four matrixes over 24 hours

		Average of 3 measurements (std. dev), nm			
Material	Hrs	LSW[A]	DMW[B]	DIW[C]	PHS[D]
10 nm	0	360.18 (46.35)	477.28 (37.13)	51.6 (2.0)	60.4 (1.9)
	24	232.70 (64.74)	356.55 (76.58)		
20 nm	0	64.25 (2.04)	71.73 (3.71)	28.3 (0.2)	36.1 (1.0)
	24	253.20 (26.33)	163.47 (21.36)		
30 nm	0	150.73 (32.70)	160.27 (7.33)	36.8 (0.2)	40.7 (0.6)
	24	173.38 (25.37)	184.57 (8.72)		
50 nm	0	177.60 (5.50)	182.48 (30.37)	51.4 (0.6)	65.8 (0.2)
	24	170.70 (5.50)	171.20 (15.90)		

[A] Filtered Lake Superior water, used as the dilution water in all toxicity tests described in this manuscript
[B] *Daphnia magna* water; 10 organisms placed in 30 mL of LSW for 24 hours, then removed
[C] Deionized water
[D] Phosphate buffer, prepared to the specifications of nanoComposix, Inc. as a stabilizer of nanosilver during storage

The increase in the DLS particle size of nanosilver is likely due to agglomeration in more complex matrixes (LSW and DMW). Nominal concentration of all samples was 2 mg L^{-1} total Ag

Table A-2 Comparison of UV-VIS absorbance characteristics of multiple sizes of nanosilver (nanoComposix, Inc.) in two experimentally relevant matrixes over 24 hours

Material	Hrs	LSW[A]		DMW[B]	
		peak AU[C]	λ, nm[D]	peak AU[C]	λ, nm[D]
10 nm	0	0.14	390	0.09	390
	24	0.08	390	0.08	390
20 nm	0	0.20	400	0.20	395
	24	0.13	400	0.15	400
30 nm	0	0.15	400	0.14	400
	24	0.11	400	0.10	400
50 nm	0	0.12	420	0.12	410
	24	0.08	420	0.09	420

[A] Filtered Lake Superior water, used as the dilution water in all toxicity tests described in this manuscript
[B] *Daphnia magna* water; 10 organisms placed in 30 mL of LSW for 24 hours, then removed
[C] Absorbance units at peak intensity
[D] Wavelength at peak absorbance intensity

The lack of a large shift in peak wavelength indicates that, although agglomerated (see Table A-1), these materials have retained their original optical characteristics after 24 hours

D. Graphite furnace atomic absorption spectroscopy analysis method for Ag quantification

Instrumentation

A Varian AA-88OZ atomic absorption spectrometer, equipped with a GTA-100Z furnace and a programmable autosampler integrated with SpectraAA-88OZ Version 5.1, was used for the analyses of Ag^{+} and nanosilver. Pyrolytically coated graphite partition tubes (Model 63-100012-00, Varian, Inc., Palo Alto, CA) were used throughout the study under the conditions shown in Table 3.

Sample preparation

Preliminary studies comparing the percent recovery of silver from a standard using a microwave digestion method and a cold acidification method revealed better recovery with the cold acidification method. For this method, samples were simply acidified to 2% HNO_3 and analyzed immediately. The automated analysis program included a rinse of the capillary tube after each reading using a 0.5% acid solution prepared from equal proportions of HNO_3 and HCl in deionized water.

Calibration

Calibration standards were prepared for each analysis using AAS Ag standard (0.999 ± 10 µg mL^{-1} in 5% HNO_3, Inorganic Ventures, Lakewood NJ) manually diluted to concentrations ranging from 1 to 50 µg L^{-1} Ag. Two absorbance readings were taken for

each sample and the average was used to make a 7-point calibration curve fit to the new rational model with the SpectraAA software.

Calculation of detection limit

The detection limit of this method is subject to bias due to the retention of Ag in the capillary tube and un-atomized Ag carried over in the furnace tube after each sample. Sensitivity was improved by the inclusion of blanks between every 8-12 samples, the addition of a high temperature clean step, increased acid concentration in the rinse solution and in the samples, and by the addition of HCl to the HNO_3 rinse solution. With these procedures in place, a series of five blanks and low standards (1 µg L^{-1}) were each read twice, and the detection limit was estimated as three times the standard error of the 10 readings taken at each concentration. This was repeated three times for each concentration, including two runs on separate days, and resulted in detection limit calculations of 9.45, 5.04, and 25.51 ng L^{-1} when measuring blanks, and 28.66, 29.85, and 40.68 ng L^{-1} when measuring low standards. Rounding up the highest value produced by this method yields a practical detection limit of 50 ng L^{-1} for the measurements reported in this document. A method detection limit of less than 10% of the lowest nominal sample concentration is generally considered acceptable (personal communication with Russ Erickson, U.S. EPA), and in Part III the lowest nominal exposure of Ag^+ to *Daphnia magna* was 0.25 µg L^{-1}, so the detection limit was only 20% of the lowest nominal sample concentration, which is higher than the optimal percentage. The Ag^+ exposures of *Pimephales promelas*, as well as nanosilver exposures of both

species, range from 3.125 to 400 µg L^{-1}, however, and so this detection limit was more than adequate for those measurements.

Table A-3 Instrument conditions for determination of total Ag in nanosilver and Ag^{+} samples with GFAAS

Varian AA 88OZ spectrophotometer

wavelength	328.1 nm
slit width	0.5 nm
lamp current	4.0 mA

GTA 100Z graphite furnace

graphite tubes	pyrolytically coated partition
sample volume	10 µl
integration mode	peak area
background correction	Zeeman

step no.	temp. °C	Time, s	gas (Ar) flow rate l/min
1	85	5.0	3.0
2	95	40.0	3.0
3	120	10.0	3.0
4	400	5.0	3.0
5	400	1.0	3.0
6	400	2.0	0.0
7	2000	0.8	0.0
8	2000	2.0	0.0
9	2000	0.1	3.0
10	2500	2.0	3.0

REFERENCES

[1] Roco MC (2005) The emergence and policy implications of converging new technologies integrated from the nanoscale. Journal of Nanoparticle Research 7: 129-143.

[2] Project for Emerging Nanotechnologies (2009) Inventory of nanotechnology-based consumer products. http://www.nanotechproject.org/inventories/consumer/

[3] Benn TM, Westerhoff P (2008) Nanoparticle silver released into water from commercially available sock fabrics. Environmental Science and Technology 42: 4133-4139.

[4] Geranio L, Heuberger M, Nowack B (2009) The behavior of silver nanotextiles during washing. Environmental Science and Technology 43: 8113-8118.

[5] Blaser SA, Scheringer M, MacLeod M, Hungerbuhler K (2007) Estimation of cumulative aquatic exposure and risk due to silver: Contribution of nano-functionalized plastics and textiles. Science of the Total Environment 390: 396-409.

[6] Luoma SN (2008) Silver nanotechnologies and the environment: old problems or new challenges? Project for Emerging Nanotechnologies, The PEW Charitable Trusts.

[7] Laban G, Nies LF, Turco RF, Bickham JW, Sepulveda MS (2010) The effects of silver nanoparticles on fathead minnow (*Pimephales promelas*) embryos. Ecotoxicology 19: 185-195.

[8] Galvez F, Wood CM (1997) The relative importance of water hardness and chloride levels in modifying the acute toxicity of silver to rainbow trout. Environmental Toxicology and Chemistry 16: 2363-2368.

[9] Bianchini A, Wood CM (2003) Mechanism of acute silver toxicity in *Daphnia magna*. Environmental Toxicology and Chemistry 22: 1361-1367.

[10] Hogstrand C, Wood CM (1998) Toward a better understanding of the bioavailability, physiology, and toxicity of silver in fish: implications for water quality criteria. Environmental Toxicology and Chemistry 17: 547-561.

[11] Wood CM, Playle RC, Hogstrand C (1999) Physiology and modeling of mechanisms of silver uptake and toxicity in fish. Environmental Toxicology and Chemistry 18: 71-83.

[12] Bar-llan O, Albrecht RM, Fako VE, Furgeson DY (2009) Toxicity assessments of multisized gold and silver nanoparticles in zebrafish embryos. SMALL 5: 1897-1910.

[13] Buzea C, Pacheco II, Robbie K (2007) Nanomaterials and nanoparticles: sources and toxicity. Biointerphases 2: 17-71.

[14] Morones JR, Elechiguerra JL, Camacho A, Holt K, Kouri JB (2005) The bactericidal effect of silver nanoparticles. Nanotechnology 16: 2346-2353.

[15] Asharani PV, Wu YL, Gong Z, Valiyaveettil S (2008) Toxicity of silver nanoparticles in zebrafish models. Nanotechnology 19: 1-8.

[16] Lee KJ, Nallathamby PD, Browning LM, Osgood CJ, Xu. XN (2007) *In vivo* imaging of transport and biocompatibility of single silver nanoparticles in early development of zebrafish embryos. ACS Nano 1: 133-143.

[17] Carlson C, Hussain SM, Schrand AM, Braydich-Stolle LK, Hess KL (2008) Unique cellular interaction of silver nanoparticles: size-dependent generation of reactive oxygen species. Journal of Physical Chemistry B 112: 13608-13619.

[18] Hussain SM, Hess KL, Gearhart JM, Geiss KT, Schlager JJ (2005) In vitro toxicity of nanoparticles in BRL 3A rat liver cells. Toxicology in Vitro 19: 975-983.

[19] Auffan M, Rose J, Bottero J, Lowry GV, Jolivet J (2009) Towards a definition of inorganic nanoparticles from an environmental, health and safety perspective. Nature Nanotechnology 4: 634-641.

[20] BSI (2007) Terminology for nanomaterials. British Standards Institution, London, UK. PAS 136:2007

[21] Handy RD, Kammer Fvd, Lead JR, Hassellov M, Owen R (2008) The ecotoxicology and chemistry of manufactured nanoparticles. Ecotoxicology 17: 287-314.

[22] Lok CN, Ho CM, Chen R, He QY, Yu WY (2007) Silver nanoparticles: partial oxidation and antibacterial activities. Journal of Biological and Inorganic Chemistry 12: 527-534.

[23] Gao J, Youn S, Hovsepyan A, Llaneza VL, Wang L (2009) Dispersion and toxicity of selected manufactured nanomaterials in natural river water samples: effects of water chemical composition. Environmental Science and Technology 43: 3322-3328.

[24] El Badawy A, Luxton TP, Silva RG, Scheckel KG, Suidan MT (2010) Impact of environmental conditions (pH, ionic strength, and electrolyte type), on the surface charge and aggregation of silver nanoparticles suspensions. Environmental Science and Technology 44: 1260-1266.

[25] Griffitt RJ, Luo J, Gao J, Bonzongo JC, Barber DS (2008) Effects of particle composition and species on toxicity of metallic nanoparticles in aquatic organisms. Environmental Toxicology and Chemistry 27: 1972-1978.

[26] Chae YJ, Pham CH, Lee J, Bae E, Yi J (2009) Evaluation of the toxic impact of silver nanoparticles on *Japanese* medaka (*Oryzias latipes*). Aquatic Toxicology 94: 320-327.

[27] Griffitt RJ, Hyndman K, Denslow ND, Barber DS (2009) Comparison of molecular and histological changes in zebrafish gills exposed to metallic nanoparticles. Toxicological Sciences 107: 404-415.

[28] Navarro E, Piccapietra F, Wagner B, Marconi F, Kaegi R (2008) Toxicity of silver nanoparticles to *Chlamydomonas reinhardtii*. Environmental Science and Technology 42: 8959-8964.

[29] Kvitek L, Vanickova M, Panacek A, Soukupova J, Dittrich M (2009) Initial study on the toxicity of silver nanoparticles (NPs) against *Paramecium caudatum*. Journal of Physical Chemistry C 113: 4296-4300.

[30] Davison W, Zhang H (1994) *In situ* speciation measurements of trace components in natural waters using thin-film gels. Nature 367: 546-548.
[31] Liu J, Hurt RH (2010) Ion release kinetics and particle persistence in aqueous nano-silver colloids. Environmental Science and Technology 44: 2169-2175.
[32] Nebeker AV (1982) Evaluation of a *Daphnia magna* renewal life-cycle test method with silver and endosulfan. Water Resources 16: 739-744.
[33] Holcome GW, Phipps GL, Sulaiman AH, Hoffman AD (1987) Simultaneous multiple species testing: acute toxicity of 13 chemicals to 12 diverse freshwater amphibian, fish, and invertebrate species. Archives of Environmental Contamination and Toxicology 16: 697-710.
[34] Naddy RB, Rehner AB, McNerney GR, Gorsuch JW, Kramer JR (2007) Comparison of short-term chronic and chronic silver toxicity to fathead minnows in unamended and sodium chloride-amended waters. Environmental Toxicology and Chemistry 26: 1922-1930.
[35] Norberg-King TJ (1989) An evaluation of the fathead minnow seven-day subchronic test for estimating chronic toxicity. Environmental Toxicology and Chemistry 8: 1075-1089.
[36] Davies PH, Goettl JPJ, Sinley JR (1978) Toxicity of silver to rainbow trout (*Salmo gairdneri*). Water Resources 12: 113-117.
[37] Ford L (2001) Development of chronic aquatic water quality criteria and standards for silver. Water Environment Research 73: 248-253.
[38] Pillai ZS, Kamat PV (2004) What factors control the size and shape of silver nanoparticles in the citrate ion reduction method? Journal of Physical Chemistry B 108: 945-951.
[39] Domingos RF, Baalousha MA, Ju-Nam Y, Reid MM, Tufenkji N (2009) Characterizing manufactured nanoparticles in the environment: multimethod determination of particle sizes. Environmental Science and Technology 43: 7277-7284.
[40] Ju-Nam Y, Lead J (2008) Manufactured nanoparticles: an overview of their chemistry, interactions and potential environmental implications. Science of the Total Environment 2008: 396-414.
[41] Maye MM, Han L, Kariuki NN, Ly NK, Chan WB (2003) Gold and alloy nanoparticles in solution and thin film assembly: spectrophotometric determination of molar absorptivity. Analytica Chimica Acta 496: 17-27.